Molecular imprinting of ACE2 Peptide Fragment: towards Development Peptide-Selective Electrochemical Sensors

Master thesis

Student: David Tsaregorodtsev 221389YASM

Supervisor: Vitali Syritski Leading Researcher

Co-Supervisor: Jekaterina Reut Senior Lecturer

Study program: YASM02/22

Tallinn 2024

ACE2 peptiidse fragmendi molekulaarne jäljendamine: peptiid-selektiivsete elektrokeemiliste sensorite väljatöötamine

Magistritöö

Üliõpilane: David Tsaregorodtsev 221389YASM

Juhendaja: Vitali Sõritski juhtivteadur

Kaasjuhendaja: Jekaterina Reut vanemlektor

Õppekava: YASM02/22

Tallinn 2024

Author’s declaration of originality

I hereby certify that I am the sole author of this thesis. All the used materials, references to the literature and the work of others have been referred to. This thesis has not been presented for examination anywhere else.

Author: David Tsaregorodtsev

27.05.2024

The paper conforms to requirements in force.
Supervisor: Vitali Syritski
[Signature, date]

Permitted to the defense.
Chairman of the Defense Committee: Ott Scheler
[Signature, date]

Abstract

Chemical and biosensors serve as analytical tools that use a recognition element as the primary sensing component coupled with a transducer to obtain analytical measurements in a convenient and user-friendly format. Synthetic molecularly imprinted polymer receptors, or MIPs, have emerged as cost-effective and stable alternatives to biological or chemical receptors. The research group of the Laboratory of Biofunctional Materials at TalTech has developed numerous MIP-based electrochemical sensors for the specific and selective detection of clinically relevant proteins, such as viral protein of SARS-CoV-2 and neurotrophic factor as BDNF. However, while most MIP technology studies focus on detecting large protein molecules, there is limited research on using short peptide sequences, which offer advantages such as lower cost, simpler structure, and greater availability compared to proteins. Therefore, the development and optimization of peptide MIP-based sensors are essential to enhance the versatility of MIP technology for detecting various targets, including proteins, and peptides.

The goal of this thesis was to study the molecular imprinting of the ACE2 peptide fragment - peptide QAKTFLDKFNHEAEDLFYQ (AM194) - to develop a peptide-selective MIP-based electrochemical sensor. This peptide, containing a sequence of 19 amino acids, was used as a model target template to prepare AM194-selective MIP (AM194 sensor). The length of AM194 was expected to be an appropriate model for synthesizing AM194-MIP film by the electrochemical surface imprinting approach. Although this imprinting approach has been used exclusively for proteins, this thesis tested its applicability for imprinting peptides of relevant lengths, highlighting the novelty of this research. It is also important to note that this study is the first to report on the molecular imprinting of the peptide sequence AM194. Initially, the appropriate functional monomer, dopamine, was selected using molecular docking modeling method. After subsequent optimization of the electrodeposition conditions, it was found that the electrodeposition of 5 mM dopamine in PBS solution by galvanostatic method at a current of 500 µA for 5.6 seconds corresponding to charge density of 5 mC/cm^2 allowed to obtain AM194-MIP with enhanced affinity to AM194. Cyclic voltammetry (CV) and differential pulse voltammetry (DPV) electroanalytical techniques were used to characterize all stages of AM194-MIP formation. The responses of the prepared AM194 sensor to the target oligopeptide at the concentration range of 1 to 100 pg/mL were determined by DPV measurements in the presence of redox probe solution. AM194 sensor demonstrated the capability to detect AM194 with a linear concentration range of 50-500 pg/mL, limit of detection of 24 fg/ml and a limit of quantitation 72 fg/ml in PBS. Additionally, it exhibited significantly higher selectivity towards AM194 compared to other peptide analogues. The obtained results lay the groundwork for future research aimed at improving peptide MIP-based sensors, which will significantly contribute to the development of cost-effective and rapid analytical tools for clinical diagnostics and environmental monitoring.

The topic is related to multiple disciplines, including electrochemistry, sensor technology, peptide detection, and molecular imprinting technology. The study was carried out in the Laboratory of Biofunctional Materials at the Department of Materials and Environmental Technology at TalTech.

Annotatsioon

Keemilised ja biosensorid on analüütilised seadmed, mis kasutavad peamise sensorkomponendina muunduriga ühendatud tundlikku elementi, et saada mugavas ja kasutajasõbralikus vormingus analüütilisi mõõtmisi. Sünteetilised molekulaarselt jäljendatud polümeeri retseptorid ehk MIP-id on kujunenud kulutõhusate ja stabiilsete alternatiividena bioloogilistele või keemilistele retseptoritele. Biofunktsionaalsete materjalide laboratooriumi uurimisrühm on välja töötanud rida MIP-põhiseid elektrokeemilisi sensoreid kliiniliselt oluliste valkude nagu SARS-CoV-2 viirusvalku ja neurotroofse valku nagu BDNF, selektiivseks tuvastamiseks. Kuigi enamik MIP-tehnoloogia uuringuid keskendub suurte valgumolekulide tuvastamisele, on lühikeste peptiidjärjestuste kasutamise kohta tehtud vähe uuringuid. Siiski pakuvad need valkudega võrreldes eeliseid, nagu madalam hind, lihtsam struktuur ja suurem kättesaadavus. Seetõttu on peptiid-MIP-põhiste sensorite arendamine ja optimeerimine hädavajalik, et suurendada MIP-tehnoloogia mitmekülgsust erinevate analüütide, sealhulgas valkude ja peptiidide tuvastamiseks.

Magistritöö eesmärgiks oli uurida ACE2 ensüümi peptiidse fragmendi - QAKTFLDKFNHEAEDLFYQ (AM194) - molekulaarset jäljendamist peptiid-selektiivse MIP-põhise elektrokeemilise sensori (AM194 sensor) väljatöötamiseks. Peptiidi AM194, mis koosneb 19 aminohapete järjestusest, kasutati mudelpeptiidina, AM194-selektiivse MIP (AM194-MIP) kile valmistamiseks. AM194 pikkus ületab veidi optimaalset peptiidi pikkust, mida tavaliselt kasutatakse molekulaarseks jäljendamiseks, kuid vastab epitoopide tüüpilisele pikkusele, mis on nende tuvastamiseks valgupinna kaudu hõlpsasti kättesaadav. AM194-MIP valmistamiseks kasutati elektrokeemilisel polümerisatsioonil põhinevat sünteesimeetodit. Kuigi seda meetodit on kasutatud ainult valkude molekulaarseks jäljendamiseks, demonstreeris see uurimistöö selle rakendatavust ka sobiva pikkusega peptiidide jäljendamiseks, rõhutades töö uudsust. Samuti on oluline märkida, et antud töös on esmakordselt kirjeldatud AM194 peptiidse järjestuse molekulaarset jäljendamist. Algselt valiti sobiv funktsionaalne monomeer, dopamiin, kasutades arvutimodelleerimist molekulaarse dokkimise abil. Seejärel viidi läbi elektropolümerisatsiooni tingimuste optimeerimist ja leiti, et galvanostaatiline sadestamine voolu tugevusel 500 µA 5.6 s jooksul, mis vastab laengutihedusele 5 mC/cm^2, 5 mM dopamiini PBS lahusest võimaldas saada AM194 suhtes suurema afiinsusega AM194-MIP kihid. AM194-MIP moodustamise kõikide etappide iseloomustamiseks kasutati tsüklilise voltamperomeetria (CV) ja differentsiaalse impulss voltamperomeetria (DPV) elektroanalüütilisi meetodeid. Valmistatud AM194 sensori võimekust AM194 selektiivseks tuvastamiseks uuriti DPV mõõtmistega redokspaari lahuse juurseolekul ja AM194 kontsentratsioonivahemikus 1 kuni 100 pg/mL. AM194 sensor oli võimeline tuvastama AM194 avastamispiiriga 24 fg/mL ja kvantifitseerimise piiriga 72 fg/mL PBS lahuses. Lisaks, näitas see oluliselt suuremat selektiivsust AM194 suhtes võrreldes teiste peptiidi analoogidega. Saadud tulemused loovad aluse peptiid-MIP-põhiste sensorite arendamisele võimaldades tulevikus pakkuda oluliselt odavamaid ja kiireid analüütilisi lahedusi kliiniliseks diagnostikaks ja keskkonnaseireks.

Magistritöö teema on seotud mitme teadusharuga, sealhulgas elektrokeemia, sensortehnoloogia, peptiidide tuvastamise ja molekulaarse jäljendamise tehnoloogiaga. Uurimistöö on teostatud Tallinna Tehnikaülikooli Materjali- ja keskkonnatehnoloogia instituudi Biofunktsionaalsete Materjalide laboratooriumis.

List of abbreviations and terms

2-ME	2-mercaptoethanol
4-ATP	4-aminothiophenol
AA	acetic acid
ACE2	angiotensin-converting enzyme 2
$Ag/AgCl/KCl_{3M}$	silver/silver chloride/3 M KCl electrode
AM160	YWDKIKDIGG peptide
AM174	YFLDAEHNFK peptide
AM194	QAKTFLDKFNHEAEDLFYQ peptide
APBA	3-aminophenylboronic acid
CE	counter electrode
CV	cyclic voltammetry
DA	dopamine
DPV	differential pulse voltammetry
DTSSP	3,3'-dithiobis[sulfosuccinimidylpropionate]
EDOT	3,4-ethylenedioxythiophene
EV233	LRRASLG peptide
mPD	meta-phenylenediamine
MIPs	molecularly imprinted polymers
NIPs	non-imprinted polymers
PBS	phosphate buffer saline
pDA	poly-dopamine
RE	reference electrode
WE	working electrode
WO	washing out

Table of contents

Introduction 9

1. Literature Review 11

1.1 Chemical and Biological sensors 11

1.1.1 Chemical sensor 11

1.1.2 Biosensors 11

1.1.3 Electrochemical sensor 12

1.2 Molecularly imprinted polymers 13

1.2.1 MIP-based electrochemical sensor 14

1.3 Peptides, synthesis and applications 15

1.3.1 Peptides as disease biomarkers in medical diagnostics 16

1.3.2 Peptides as imaging or diagnostic probes 17

1.3.3 ACE2 peptide fragment 17

1.3.4 Classical methods for peptide detection 18

1.4 Molecular imprinting of peptides 19

1.4.1 Epitope imprinting 19

1.4.2 Peptide MIP-based sensor 20

1.5 Electrochemical methods for analysis 20

1.5.1 Cyclic voltammetry 20

1.5.2 Differential pulse voltammetry 22

1.6 Aims 23

2. Experimental part 24

2.1 Chemicals and materials 24

2.2 Electrochemical measurements 24

2.2.1 Cyclic voltammetry 25

2.2.2 Differential pulse voltammetry 25

2.3 Functional monomer selection 25

2.3.1 Molecular docking of AM194 25

2.4 Synthesis of AM194-MIP 25

2.4.1 Functionalization and immobilization 26

2.4.2 Electrodeposition of poly-DA 26

2.4.3 Peptide removal 27
2.5 Performance of AM194 sensor 27
2.5.1 Rebinding study 27
2.5.2 Selectivity study 28
3. Results and discussion 29
3.1 Selection of functional monomer 29
3.2 AM194-MIP preparation 30
3.2.1 Characterization of AM194-MIP preparation stages 30
3.2.2 Optimization of pDA electrochemical synthesis 31
3.3 AM194 sensor performance study 33
3.3.1 Binding isotherm analysis 34
3.3.2 Sensitivity of AM194 sensor 35
3.4 Selectivity study 36
4. Conclusions 38
Acknowledgments 39
References 40
Appendix 1 50
Appendix 2 51

Introduction

Sensors of different types, such as chemical and biosensors, are increasingly used in various areas, including medicine, environmental or food quality monitoring[1,2]. The main sensitive material, or recognition element, of a biosensor is based on bioreceptors, which are selective, but at the same time very unstable and expensive. In recent years, molecularly imprinted polymers (MIPs) have been widely studied as an alternative for unstable bioreceptors. MIPs are synthetic materials designed to recognize target molecules with high affinity and specificity[3,4]. MIPs are formed by embedding and subsequent removal of the three-dimensional structure of a target molecule into a polymer matrix. The resulting MIPs have molecular binding sites that complement by the size, shape, and arrangement of functional groups to the target molecule. Integration of MIP materials in to sensing platform allows to create MIP-based sensors, which have been extensively studied due to their potential for application across various domains, including viruses and water pollutants detection[5,6].

Peptides, which are chains of amino acids linked by peptide bond that contain from a couple to 50 amino acids[7,8], play a key role in biological processes, acting as signaling molecules, drug targets, fluorescent diagnostic probes and biomarkers of various diseases[9,10]. Their unique biochemical properties make them valuable tools in biomedical research and clinical diagnostics. The property of peptides to specifically bind to certain proteins, viruses or enzymes is of great interest for studying their mechanisms of binding to specific macromolecules and regulation of enzymes.

Therefore, finding a facile method to generate peptide-selective MIPs has gained significant attention in the field of molecular imprinting. Targeting MIP-based sensors directly to detect peptides of needed sequences of amino acids, demonstrating their potential for use as biosensors, drug delivery, or disease monitoring[11,12]. It should be noted that according to the previous reports, peptides ranging from 7 to 12 amino acids in length have been recognized as the optimal size for to achieve successful imprinting[13].

The development of selective and sensitive sensors for peptide detection would advance the use of chemical or biosensors in various fields including medicine. Electrochemical, thermal, or optical sensors can be used as a basis transducer principle, depending on the areas and purposes being studied. The electrochemical sensor will be used in this thesis because of its advantages: it is simple, cheap and has high sensitivity[14].

This master thesis aims to study the molecular imprinting of the ACE2 peptide fragment - peptide QAKTFLDKFNHEAEDLFYQ (AM194) - to develop a peptide-selective MIP-based electrochemical sensor. This peptide, containing a sequence of 19 amino acids, can be used as a model target template to prepare AM194-selective MIP (AM194-MIP). The length of AM194 slightly exceeded the optimal peptide length usually employed for imprinting but corresponds to the typical length of epitopes readily accessible for their recognition via protein surface. Thus, AM194 is expected to be an appropriate model for synthesizing AM194-MIP film by the electrochemical surface imprinting approach[5]. Although this imprinting approach has been used exclusively for proteins, this thesis tested its applicability for imprinting peptides of relevant lengths, highlighting the relevance and novelty of this research. It is also important to note that this study is the first to report on the molecular imprinting of the peptide sequence AM194.

To achieve the goals of the thesis, firstly, it is necessary to select the appropriate functional monomer and optimize its electrochemical polymerization and following AM194-MIP formation in order to maximize the binding affinity between the AM194-MIP and AM194. Then, to study the capability of the electrochemical sensor consisting of AM194-MIP layer integrated with the electrode (AM194 sensor) to selectively rebind AM194 by measuring the electrochemical responses in the relevant solutions containing AM194. Furthermore, the ability of the sensor to discriminate between AM194 and similar peptides. The success of these studies would make a substantial contribution to the development of sensitive and selective MIP-based sensors capable of detecting peptides of varying sizes and chemical properties.

1. Literature Review

1.1 Chemical and Biological sensors

1.1.1 Chemical sensor

Chemical sensors are important analytical tools in many areas, including monitoring industrial production processes, public security, and medicine[15–17]. The development of portable, sensitive, low-power consumption and cost-effective sensors is very demanded. A chemical sensor converts chemical data, such as composition, concentration, or the presence of a certain element, into an analytically useful signal[18]. Typically, it is composed of two components: a transducer and a recognition element or receptor (Figure 1). The sensory material, as a recognition element, is crucial for the receptor part due to its capacity to transform the interaction between the studied analyte and the sensory material into a physical parameters[18]. The recognition element of a chemical sensor is responsible for interacting with the target analyte, leading to a consequential change in material properties, such as mass, concentration, or electrical conductivity. The transducer, on the other hand, converts the physical attribute into an appropriate electrical signal and regulates the signal's intensity. Ensuring seamless coordination between these components is imperative for optimal sensor performance across various applications.

1.1.2 Biosensors

Chemical sensors that use a biological receptor as a recognition element are called biosensors. The biological recognition elements are usually enzymes, antibodies or nucleic acids[19]. Biosensors can measure and identify biological components such as proteins, nucleic acids, viruses or cells[20,21]. They play an important role in various fields including medicine, food science and environmental monitoring[22]. Biosensors is composed of two components, same as chemical sensors, however as recognition element some biological material is used, which utilizes a biochemical mechanism[23–25]. The biological interaction between the bioreceptor and analyte is converted through the transducer into a quantifiable signal that is then translated into an observer-understandable signal. Same as chemical sensors, biosensor have amplifier, that increases the power of a signal, then transformed signal is measured by a detecting device before being sent to the processor, which projects the desired outcome in the form of graphs or numbers on the screen[26]. Depending on the signal transduction mechanism there are different types of chemical and biosensors, such as electrochemical[27], optical[28], piezoelectric[29] and thermal sensors[30]. In this thesis an electrochemical sensor will be utilized.

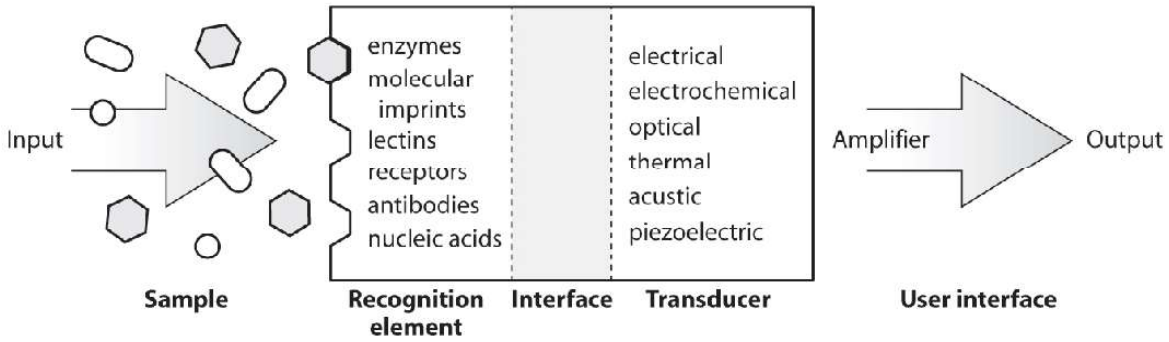

Figure 1. Schematic working design of chemical and biosensor (adapted from [31]).

1.1.3 Electrochemical sensor

Electrochemical sensors are special devices that convert the effect of the electrochemical interaction analyte-electrode into a useful analytical signal[18]. Such effects can be electrically stimulated or lead to a spontaneous interaction in the zero-current condition. In this kind of chemical sensors, an electrode acts as a transducer[32]. Electrochemical sensors have many advantages, such as high sensitivity, fast response, simplicity, ease of miniaturization and low cost[14].

Electrochemical sensors are integral components of an electrochemical cell, which can feature either three electrodes or two electrodes[33]. In a standard three-electrode electrochemical cell (Figure 2), there is a working electrode (WE) composed of a chemically stable solid, conductive material such as platinum, gold, or carbon; a reference electrode (RE) typically constructed from silver metal coated with a layer of silver chloride (Ag/AgCl); and a counter electrode (CE) made of platinum wire. In an electrochemical sensor, the working electrode is modified with biological or synthetic recognition layer that possesses the capability to establish a stable complex with the target molecule present in the analyte solution.

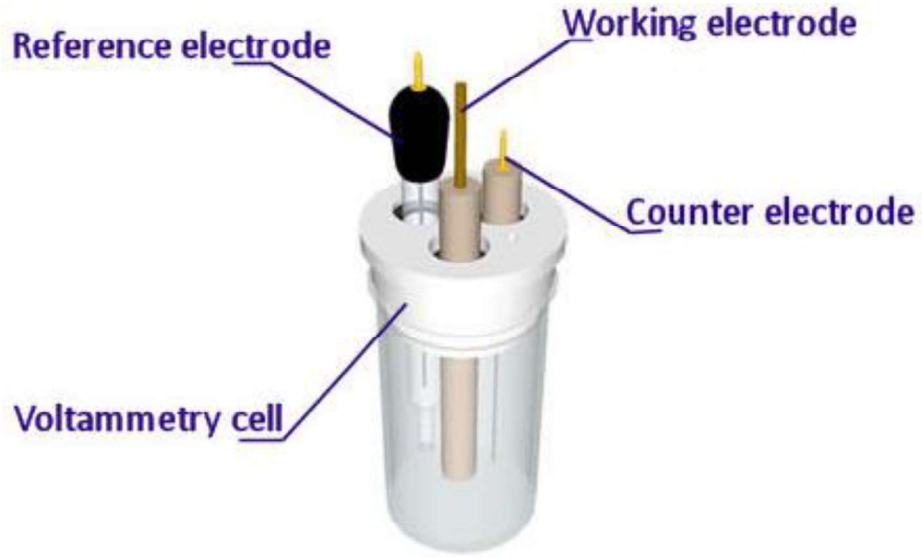

Figure 2. Three-electrode electrochemical cell[34].

These electrochemical sensors can also be used for Point-of-Care Testing (PoCT), for low-cost use and fast test results in a patient-friendly environment[35]. PoCT devices offer an alternative to large medical laboratories, where obtaining a sample, conducting time-consuming and costly experiments, and waiting for results often delay necessary treatments. Examples of electrochemical transducers suitable to fabricate sensor devices in PoCT format include Screen Printed Electrodes (SPEs) and Thin-Film Electrodes (TFEs). SPEs offer high sensitivity and miniaturized low-cost transducers, with a key advantage being the reduced sample volume required for *in situ* analysis (Figure 3a)[36]. This volume can be as low as a few microliters, and SPEs can conveniently integrate into portable potentiostats. However, SPEs are single-use only due to the possibility of destructive reactions with organic solvents with its unstable WE surface. On the other hand, TFEs utilize thin-film technology, using vacuum filtration methods or growing metal layer on an electrode material, which serve as an electrochemical transducer and composed of metal layer that ranges in thickness from nanometers to micrometers (Figure 3b), but organic materials, despite having well-defined

porous structures and redox activity, may exhibit poor conductivity, affecting the overall efficiency[37].

(a) 

(b) 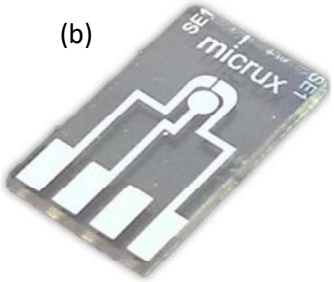

Figure 3. (a) Screen-Printed Electrodes[38] and (b) Thin-Film Electrodes[39].

Two primary categories of electrochemical sensors include amperometric and potentiometric sensors[40]. Potentiometric sensors involve the measurement of potential difference between the reference electrode and the working electrode without inducing polarization of the electrochemical cell, thereby allowing only minimal current flow[14]. In contrast, amperometric sensors utilize a potential applied between a reference and a working electrode to facilitate the oxidation or reduction of an electroactive species, with the resulting current being measured[41]. This electric current is influenced by the electrochemically active analyte particles undergoing oxidation or reduction at the surface of the working electrode, with the sensor signal demonstrating a linear relationship with the analyte concentration. Electrochemical techniques are particularly well-suited for directly quantifying redox analytes in solution and for determining redox enzymes or their analogues by monitoring the formation of electroactive products[42]. Moreover, electrochemical sensing methods can be effectively employed for non-electroactive targets through indirect detection approaches, wherein changes in the electrochemical signal of an external electroactive compound or redox probe are recorded upon interaction with a molecular recognition layer present on the electrode surface[43].

1.2 Molecularly imprinted polymers

Nevertheless, despite the considerable advancements in biosensor development, a significant limitation persists, primarily stemming from the labile nature, environmental instability of biological receptors, as well as their costly and time-consuming production processes[44,45]. Thus, It is important to find a suitable technology to produce robust and cost-effective synthetic receptors while ensuring the highest sensitivity and specificity[46].

Synthetic receptors based on molecularly imprinted polymers (MIPs) have been developed and studied over the past decades as a promising alternative to unstable bioreceptors in sensors. These polymers are engineered to mimic the molecular structure of a target molecule that was used as a template during the MIP synthesis[3]. Generally, a MIP synthesis procedure includes the following steps: covalent or non-covalent complex formation between a functional monomer and a template molecule; polymerization; template removal from the polymer, leaving binding cavities that a complementary to the template molecule in size, shape, and arrangement of functional groups (Figure 4). The resulting MIP has high affinity and specificity for the target analyte, granting MIP-

based receptors the ability to recognize and bind to the analyte in the studied environments. MIPs as recognition elements can be integrated with various sensor platforms aiming in detection and analysis of a wide range of analytes ranging from the small molecules such as amino acids, single molecules, antibiotics, pesticides to a macromolecules such as proteins, virus and cell[4,47–49].

MIP-based sensors are pivotal in numerous research domains, spanning medicine and environmental protection. For example, in medicine, MIP sensors are very promising analytical tool for diagnostics of various diseases such as SARS-CoV-2[5], Alzheimer's disease[50] or other neurodegenerative diseases[51]. In environmental monitoring, MIPs are useful instruments for evaluating the state of the environment and making it easier to quickly identify pollutants[4,6].

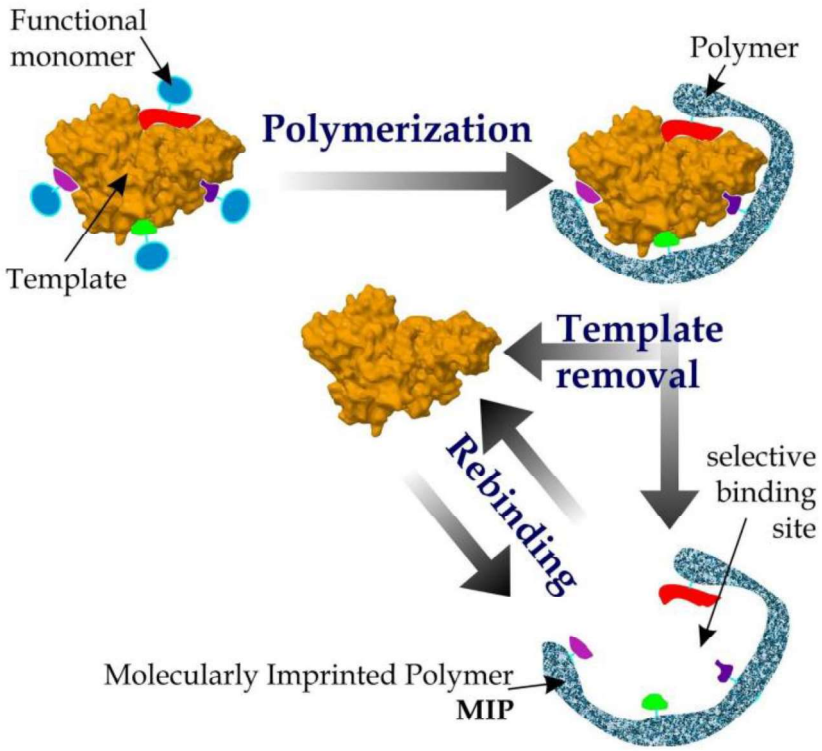

Figure 4. A general scheme of MIP synthesis[52].

1.2.1 MIP-based electrochemical sensor

The favorable attributes of electrochemical sensors based on MIPs include ease of use, rapid response, high sensitivity, cost-effectiveness, and suitability for customization to meet diverse clinical monitoring, food technology or environment monitoring needs[53].

In the general context of MIP-based electrochemical sensors, the transduction mechanism depends on the inherent properties of the analyte. Direct transduction occurs when the redox processes of the target analyte itself and its redox-active products are monitored. Indirect transduction is used when the target analyte is non-electroactive, and the change in the signal of an external redox probe is monitored. While direct oxidation-reduction of an analyte on the MIP-modified sensor has been reported in some studies[54], the indirect method is more commonly utilized for non-electroactive analytes. In this approach, the electrochemical readout relies on the "gate effect", which occurs due to the occupancy of imprinted cavities within the MIP by analyte molecules. The presence of analyte molecules obstructs the diffusion of small redox probes, thereby impeding

charge transfer at the electrode/solution interface and resulting in a reduction in redox current[55]. The reversible redox pair $K_3[Fe(CN)_6]/K_4[Fe(CN)_6]$ is frequently employed as a redox marker to monitor the indirect response of MIP-based electrochemical sensors[43].

During the measurement process, the intensity of the current resulting from the redox reaction of $K_3[Fe(CN)_6]/K_4[Fe(CN)_6]$ at the MIP-based sensor surface is monitored. In the absence of analyte molecules bound within the imprinted cavities of the MIP, the redox probe ions can freely move at the electrode/solution interface, resulting in the highest current peak intensity, as indicated by the blue line in Figure 5. However, if the film has bound its target molecule following incubation of the sensor in a sample solution, the charge transfer is efficiently hindered, leading to a decrease in current, as depicted by the red line in Figure 5. This decrease in current is correlated with the concentration of the analyte in the solution.

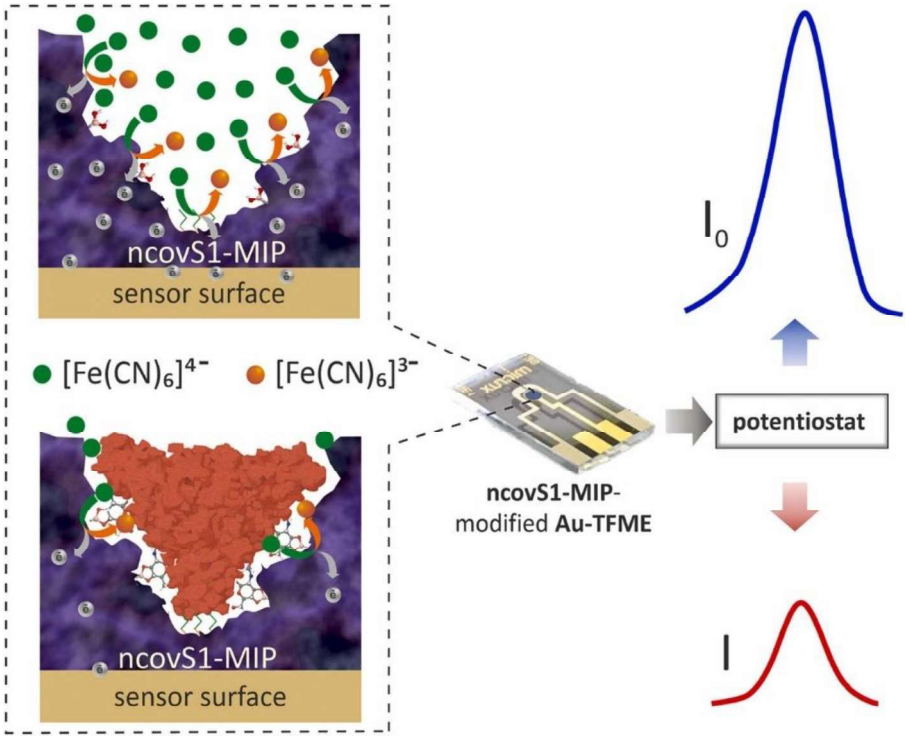

Figure 5. The operating principle of a MIP-based electrochemical sensor exemplified for a sensor detecting SARS-CoV-2 spike protein (ncovS1)[56].

1.3 Peptides, synthesis and applications

Peptides, consisting of amino acid residues, exert significant influence on numerous physiological processes within the human body[8]. Amino acids are organic compounds characterized by the presence of an amino group ($-NH_2$) and a carboxyl group (-COOH). Peptide bonds arise through the linkage of two successive amino acids between their C1 and N2 atoms, leading to the creation of extensive chains comprising amino acid residues, along with water molecules as a side product. Long peptide sequences, consisting of 20 different amino[57], can form extensive chains linked by peptide bonds. Peptides with chains of consecutive amino acids ranging from a couple to 20 are called oligopeptides, with a longer sequence length they are called polypeptides, that can be formed into proteins, starting from the primary structure, up to the quaternary. The mechanism of

peptide bond formation resulting from the interaction between two amino acids is depicted in Figure 6.

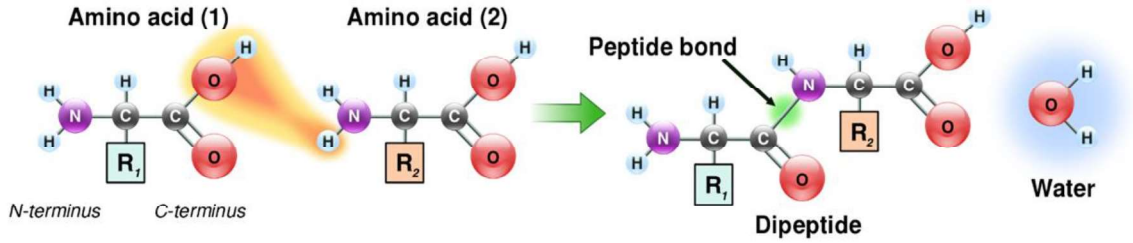

Figure 6. Peptide bond formation via dehydration reaction scheme (adapted from [58]).

There are several methods for synthesis of peptides of different sizes and different amino acid sequences. One of the most widely used synthesis methods is solid-phase peptide synthesis (SPPS)[59]. The SPPS method is based on the rapid assembly of peptide chains through sequential reactions of amino acid derivatives on a macroscopically insoluble granular resin solid support. This solid support consists of small polymer resin beads, functionalized with reactive amine or hydroxyl groups binding to the formed peptide chain. The peptide remains covalently bound to the solid support throughout the synthesis, where side products are removed by washing and filtration processes. This approach avoids the relatively time-consuming isolation of the peptide product from solution after each reaction step, which would be required using traditional solution synthesis[60].

The deep interest in the study of peptides stems from their unique biological properties and the potential medical applications of these peptides. For example, a huge number of peptides are used in medicine as drugs. These peptide drugs are called therapeutic peptides[9,61]. Research into the use of therapeutic peptides began with the study of natural human hormones such as insulin, oxytocin and vasopressin[9]. Considering the length of known peptide hormones, then most of them have a length from 7 to 13 amino acids in sequence[62]. In recent years, therapeutic peptides have become one of the major pharmaceutical industry products and more than 60 peptide drugs based on therapeutic abilities have been released[63] including: hormonal peptides[62], antimicrobial peptides[64], anticancer peptides[65], neuropeptides[66] and immunomodulatory peptides[67]. They can modulate physiological processes, inhibit or activate enzyme activity, and interfere with protein-protein interactions that are involved in disease progression[68]. In our everyday life, peptides of different sizes are widely used in such fields as cosmetology, medicine, ecology, food industry and infectious safety[69]. Peptides can be used as disease biomarkers[70,71], recognition elements of biosensors[72] as well as to produce vaccines[73].

1.3.1 Peptides as disease biomarkers in medical diagnostics

A biomarker, is a measurable indicator that can be used to assess an organism's physiological state, disease processes, or response to therapy[74]. Biomarkers can be molecular, cellular or tissue and can be measured in various biological materials, such as blood, urine, saliva or tissues[74]. Peptide biomarkers often have higher specificity for certain biological processes or pathological conditions and can be more sensitive to changes in the body, making them useful for early diagnosis or monitoring of diseases[75]. Examples of peptide biomarkers include cancer peptides that are used as biomarkers for early detection of cancer[76] and other peptide biomarkers, playing an crucial role in the detection of Alzheimer's disease[77]. In other research, one group of scientist studied the main

antimicrobial peptides, which identified in the epidermal mucus of the fish species, and these peptides have potential as biomarkers for antimicrobial activity in fish mucus[78].

1.3.2 Peptides as imaging or diagnostic probes

Peptides labeled with imaging moieties can serve as diagnostic probes in targeted molecular imaging, facilitating early disease detection, monitoring of therapeutic responses, and evaluation of drug efficiency[79]. Molecular imaging is a field of medical imaging that focuses on visualizing molecules of medical interest in patients *in vivo*. For this method, peptides conjugated with imaging moiety with a short half-life (for instance ^{19}F or ^{99m}TC) through covalent bonds. The imaging moiety can be an organic dye or a radioactive nuclide. Then these moieties are visualized in the patient's body through various tomography methods (PET, SPECT, MRI and etc.)[80]. The tomography results-images show how certain areas have higher color activity than others, which indicates the presence of peptides in these points, intended for molecular imaging.

Peptide molecules that have previously been labeled with a fluorescent dye, or fluorescent peptide, are able to emit light at a specific wavelength. Click chemistry can be used to conjugate fluorescent dyes to peptides[81]. The alkyne in the peptide and the azide in the dye react with one another in the click chemical reaction when Cu is present as a catalyst. This method is selective, fast, efficient and the reaction takes place in ordinary water, making it a basic and simple method for producing fluorescent peptides[82]. The detection of fluorescent peptides in modern biomedicine offers promising avenues for accurate and sensitive analysis methods, facilitating visualization and monitoring of biological processes at cellular and molecular levels[83]. Their unique optical properties enable highly sensitive and specific detection, making them valuable tools for studying protein-peptide interactions and diverse biological and medical applications, including visualizing biological structures, detecting biomolecules, and labeling cells and proteins[84]. In the field of diagnostics, the use of these peptides offers the possibility of early detection of various diseases such as cancer and infections[71,85].

1.3.3 ACE2 peptide fragment

This thesis focuses on the molecular imprinting of an oligopeptide QAKTFLDKFNHEAEDLFYQ[86] (AM194), as a model peptide to prepare a MIP-based electrochemical sensor for selective peptide detection. AM194 represents a peptide fragment of the angiotensin-converting enzyme 2 (ACE2), that is a critical element in regulating the renin-angiotensin-aldosterone system[87]. This membrane glycoprotein has a significant role in maintaining homeostasis in the human body[88]. ACE2 is a Zn-containing metalloenzyme that consists of 805 amino acids with a molecular weight of 120 kDa (Figure 7)[89]. ACE2 is expressed in most tissues, such as on the cell membranes of arteries and veins, as well as on muscle cells in most organs. In addition, this enzyme was also found in the cells of the cerebral cortex, the presence of which indicates possible neurological diseases in the absence of ACE2 protein[90].

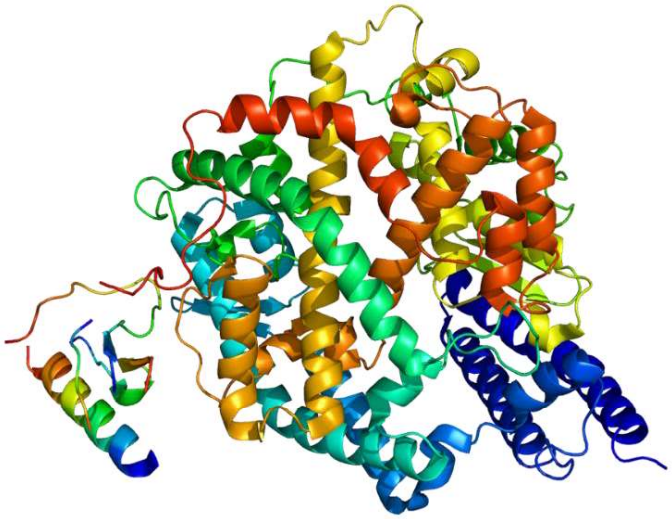

Figure 7. Structure of the ACE2 protein[91].

The laboratory of Institute of Chemistry at Tartu University synthesized and studied a peptide fragment of the ACE2 protein - AM194[86] (Figure 8b). AM194 is a peptide sequence containing 19 amino acids of the α1 domain of the N-terminal part of ACE2 molecule, which has a molecular weight of 2.3 kDa. This oligopeptide is an important part of the binding of the enzyme ACE2 and S1 protein of SARS-CoV-2 virus[86] and was used to determine the minimal amino acid sequence in the ACE2 enzyme that interacts with the SARS-CoV-2 virus. The length of AM194 was determined as the ”minimal sequence“ needed for ACE2 recognition by the receptor binding domain (RBD) on the S1 protein of SARS-CoV-2[86].

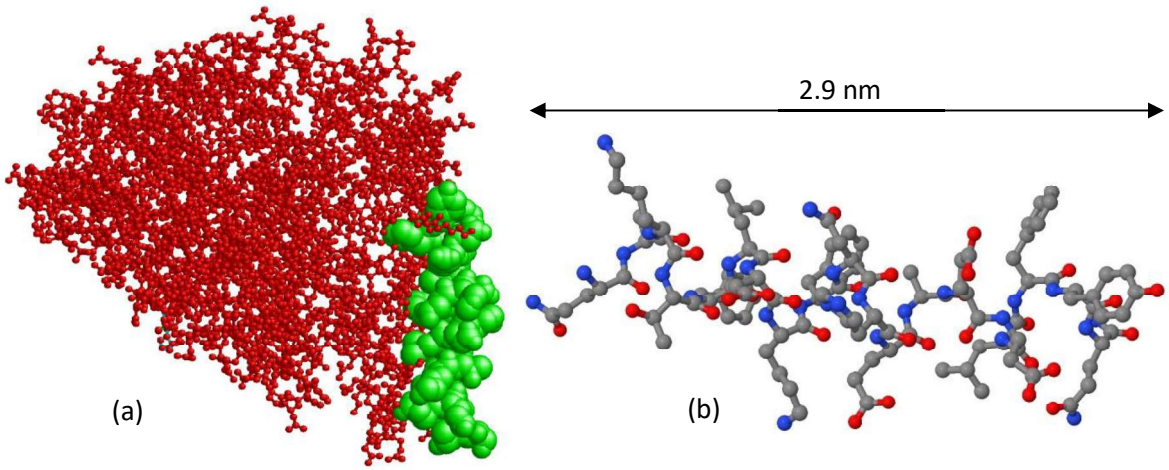

Figure 8. (a) Peptide sequence (green), containing amino acids 19-45 of the α1 domain of the N-terminal part of ACE2 molecule (red) and (b) ball-and-sticks model of AM194 peptide and its approximate length. These models were visualized with JMol-16.1.53 Software.

1.3.4 Classical methods for peptide detection

Various methods have been used to identify and quantify peptides in biological samples. One commonly used technique is enzyme-linked immunosorbent assay (ELISA), which relies on the specific binding of antibodies to peptides of interest. In the ELISA procedure, a target macromolecule, or antigen, is immobilized on a solid surface and a specific antibody attached to a reporter enzyme complexes with it thereafter. Detection is accomplished by incubating the

appropriate substrate with the reporter enzyme and measuring its activity to generate a quantifiable result[92]. ELISA offers high sensitivity and specificity, making it suitable for detecting peptides in complex biological samples[93]. Another method is mass spectrometry (MS), which involves ionizing peptides and measuring their mass-to-charge ratios. MS provides accurate identification and quantification of peptides, especially in proteomic studies[94]. Additionally, chromatographic techniques such as high-performance liquid chromatography combined with MS or gas chromatography can separate peptides based on their physicochemical properties, allowing for their detection and quantification[95,96]. Overall, the choice of method for peptide detection depends on factors such as sample type, peptide concentration, and required sensitivity and specificity. Primarily because peptides are present in low concentrations in biological samples, their detection can be complicated, in the presence of other molecules in the sample that can create background noise or cross-react with the peptides. Another problem is the sequence variability, similar chemical composition, and structures which can cause difficulties in developing universal detection methods. However, ongoing research and innovation in peptide detection methods is gradually overcoming these difficulties, expanding the possibilities of using peptides in research, biotechnology or medicine.

1.4 Molecular imprinting of peptides

In recent years, many applications of the MIP technique have been explored to create peptide-selective polymers-peptide MIPs. Especially, MIP nanoparticles have been extensively studied for detection of peptide with different sequences as well as proteins[97]. These “plastic antibodies” have a huge potential to contribute towards biomedical applications aiming at biosensors, drug delivery and etc[11,12,98]. However, peptide size and amino acid sequence are important factors to consider while synthesizing a peptide MIP-based electrochemical sensor, since they can have an impact on the interaction process with polymer matrix and functional groups. Depending on the nature of the target analyte molecular imprinting of peptides can be approached in two directions: epitope-imprinting, for MIP intended to detect protein, and peptide-imprinting, for MIP detecting peptides. These methods will be considered more closely in the following sections.

1.4.1 Epitope imprinting

Epitope-imprinting are a fascinating area of research within the field of MIPs aiming to address challenges and limitations of protein imprinting, such as complexity of protein structure, template removal difficulties, limited stability, reusability and template availability[99]. Epitopes represent small functional segments of an antigenic protein, which are recognized by the immune system. Typically comprising 9-15 amino acid residues, epitopes are localized on the protein's surface. The challenges associated with MIP imprinting macromolecules from their intricate structure, flexibility, and high production expenses. In epitope imprinting, these antigenic epitopes serve as templates for creating cavities within a polymer matrix, offering a more convenient and cost-effective alternative MIPs. By using a smaller compound as the template, the structural and cost issues previously associated with larger molecules can be circumvented, while still retaining selective recognition and affinity for the larger target. By imprinting epitopes onto polymers, researchers can develop synthetic receptors that emulate the binding specificity observed in natural antibodies[100,101]. Epitope-MIP based sensors present several advantages over conventional antibody-based sensors, including enhanced stability and affordability, rendering them appealing

for diverse applications in diagnostics, biomarker detection, and disease monitoring[99]. Examples of epitope-imprinting include researches in which nanoparticles were synthesized based on the p32[102] protein epitope. One key challenge in developing epitope-MIPs is ensuring that the imprinted epitopes retain their structural integrity and binding affinity within the polymer matrix. The choice of functional monomers, and the imprinting process all play crucial roles in determining the performance of epitope-MIPs in detecting target proteins[101]. Moreover, it was found that the size of the epitope should not exceed 16 amino acids in sequence, as it may start to undergo intramolecular interactions and negatively influence their interactions with polymers of the MIP[101].

1.4.2 Peptide MIP-based sensor

Peptide-selective MIPs were also developed with the aim of recognizing a specific peptide as a target analyte. For instance, a MIP designed for the hormone oxytocin was synthesized using bulk polymerization, with a tetrapeptide representing the C-terminal section of oxytocin as the template[103], similarly it is also possible to synthesize selective MIPs towards peptides such as EGFR peptide[104] and carnosine[105]. It should be noted that to achieve successful imprinting of the peptide, it is important to select the optimal peptide sequence length. The peptide should neither be too short, which may lead to similar sequences, nor too long, because longer sequences will fold and constantly change their position in imprints, and this could cause imprinting issues. Peptides ranging from 7 to 12 amino acids in length have been recognized as the optimal size for synthesizing highly selective MIPs[13]. However, a study involving the synthesis of MIPs based on the toxic peptide melittin (MEL), which spans 26 amino acids in length, indicates the potential for utilizing peptides of varying lengths in MIP synthesis[106,107].

There are several reports on the peptide-MIP based electrochemical sensors[108,109]. In the first study, tripeptide was used as a functional group that was immobilized onto gold WE surface through an Au–S bond. This immobilization allowed the tripeptide to interact with vancomycin in solution and form analyte-peptide complexes. Subsequently, a controlled electrodeposition of functional monomer was carried out to imprint the vancomycin-tripeptide complexes, creating hybrid peptide-MIP cavities containing multiple binding sites for vancomycin on the electrode surface[108]. In the second study, peptides from the receptor-binding domain on the SARS-CoV-2 spike protein, with 10 amino acids in sequence, were used as an analyte and imprinted onto the working surface of indium tin oxide (ITO) electrode with the addition of Ti_2C to increase the electrochemical response[109].

1.5 Electrochemical methods for analysis

1.5.1 Cyclic voltammetry

Cyclic voltammetry (CV) is a powerful and versatile electrochemical technique used to study the electron transfer processes occurring at an electrode surface[110]. It involves applying a potential waveform that sweeps linearly between a set starting potential (E_1) and a final potential (E_2), and then back to the starting potential[111,112]. The current response (I) is measured throughout the potential sweep, resulting in a characteristic plot known as a CV voltammogram. CV is the effective electroanalytical technique that can be used to study electrical charge transfer from redox probe solution to electrode surface and study blocking properties of MIP-based sensors[48]. During a CV experiment, the applied potential drives the redox reaction at the electrode. As the potential is

scanned, the concentration of oxidized and reduced species at the electrode surface changes. This change in concentration affects the current flow, leading to the oxidation and reduction peaks in the CV[111,113]. On Figure 9 we can observe the 4 main parameters: the potential of the anodic (E_{pa}) and cathodic (E_{pc}) peaks, and intensity of peak currents of the anodic (i_{pa}) and cathodic (i_{pc}) peaks.

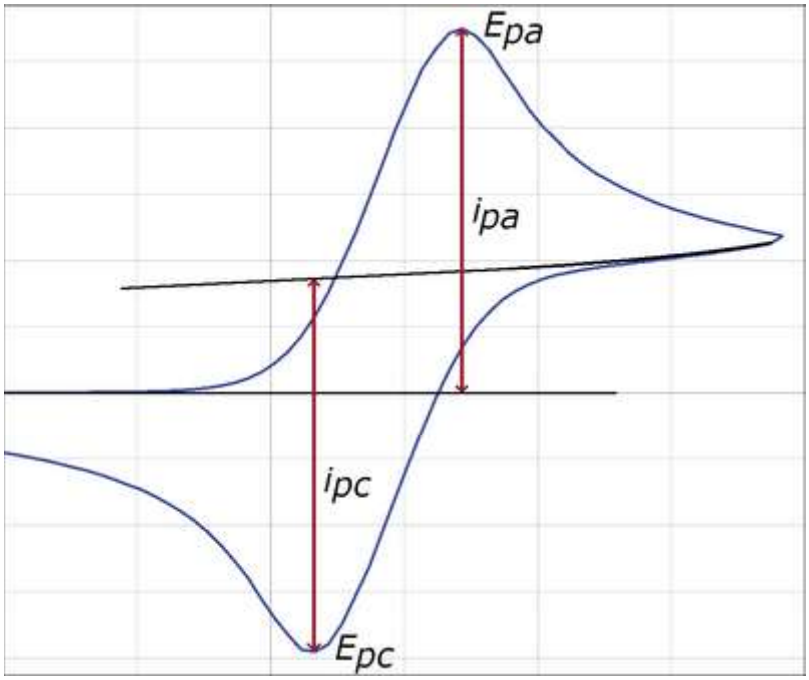

Figure 9. Simplified scheme of cyclic voltammogram, where E_{pa} is an anodic peak potential, E_{pc} is a cathodic peak potential, i_{pa} is an anodic peak current and i_{pc} is a cathodic peak current[114].

The CV method serves not only to observe the redox process, but it can also be used to generate conducting polymer layers as transducers for sensors by cycling between potentials at which the polymer is formed[115]. The thickness and morphology of conducting polymer films can be effectively regulated by modifying the electrochemical parameters and the composition of monomer solutions during the cyclic potentials application. At the same time CV technique provides valuable insights into the dynamic interaction between biomolecules and the electrode surface. By measuring the current response as a function of the applied potential, CV reveals the electrochemical behavior of biomolecules, including their oxidation and reduction processes. The appearance of anodic peaks corresponds to the oxidation of biomolecules, while cathodic peaks indicate their reduction[116–119].

From these potentials an important parameter is calculated, which shows the formal potential (E^0) (Equation 1.1), which is an important criterion for the Nernst equation[120] (Equation 1.2).

$$E^0 = \frac{E_{pa}+E_{ca}}{2}, \qquad \text{(Equation 1.1)}$$

and this potential is used further to calculate the value of the electrode potential (E)

$$E = E^0 - \frac{RT}{\mathrm{zF}} * log\frac{[Ox]}{[Red]}, \qquad \text{(Equation 1.2)}$$

where E is the electrode potential, E^0 is the formal potential, R is the universal gas constant (8.314 J/K·mol), T is the temperature (K), z is the number of electrons transferred, F is the Faraday's constant (96485 C/mol), *Ox* and *Red* is the oxidized and reduced electrodes in the CV system.

1.5.2 Differential pulse voltammetry

While cyclic voltammetry (CV) offers a powerful tool for studying electrochemical reactions, it has limitations in terms of sensitivity, particularly for analytes present in low concentrations. Differential pulse voltammetry (DPV) emerges as a refined technique that addresses this challenge. DPV builds upon the principles of CV but incorporates a pulsed potential waveform to enhance the signal-to-noise ratio and improve detection limits[121,122]. DPV utilizes a staircase potential waveform superimposed on a linear potential sweep (Figure 10). The staircase waveform consists of a series of small potential pulses applied at regular intervals[123]. The current is measured just before each subsequent pulse. During the pulse application, charging currents associated with the double layer capacitance at the electrode interface are minimized. By measuring the current just before the next pulse, the contribution of these non-faradaic currents is significantly reduced. At the same time by sampling the current at specific points, DPV effectively filters out random fluctuations in the background current, leading to a cleaner signal and enhanced sensitivity for the faradaic current associated with the analyte's redox reaction[124,125]. Figure 11 shows a typical DPV voltammogram consisting of the plot of recorded current versus the applied pulse potential. This current peak of DPV is directly proportional to the concentration of the analyte, and based on DPV voltammograms, it is possible to describe the interaction between sensor and analyte[126,127].

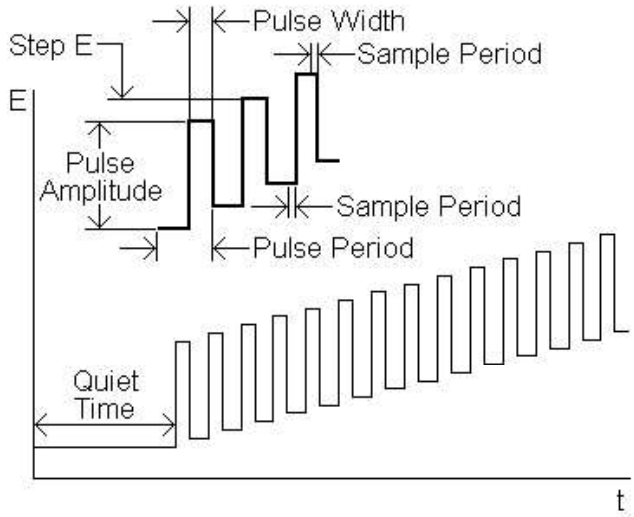

Figure 10. Staircase potential waveform form DPV[123].

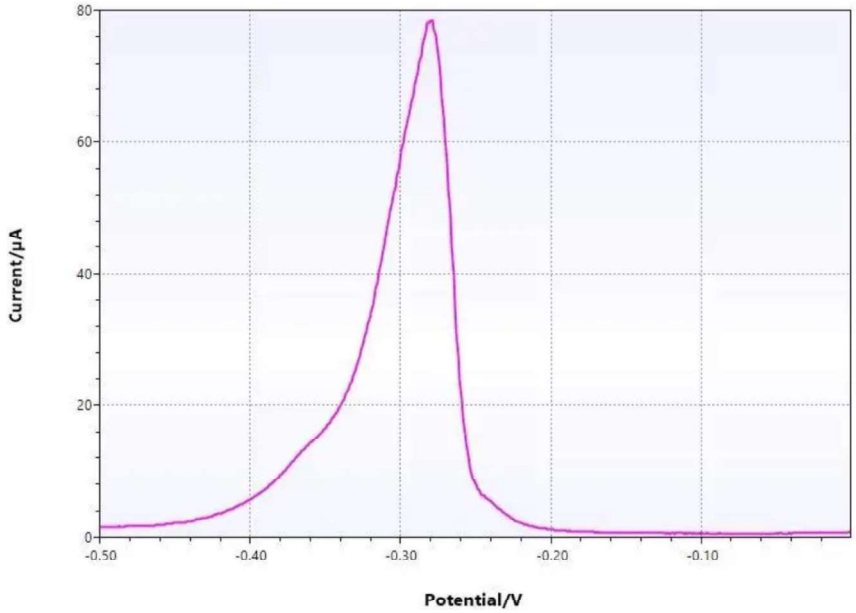

Figure 11. The typical DPV curve showing the change in visible current vs pulse potential[128].

1.6 Aims

The main aim of this thesis was to study the molecular imprinting of AM194, to develop a peptide-selective MIP (AM194-MIP) and its subsequent integration with an electrode in order to build AM194 electrochemical sensor. AM194 containing 19 amino acids, representing a peptide fragment of the ACE2 enzyme, was selected as a model peptide with length of interest. According to the literature, the imprinting of peptides is typically limited to sequences between 7 and 12 amino acids. The novelty of this thesis lies in the imprinting of a longer peptide (AM194), which adds complexity to the imprinting process but may provide enhanced selectivity for the resulting peptide-MIP-based sensors and extend the range of target peptides in MIP-based sensing.

To achieve the aim of the thesis, firstly, it is necessary to select the appropriate functional monomer and optimize its electrochemical polymerization and following AM194-MIP formation in order to maximize the binding affinity between the AM194-MIP and AM194. Then, to study the capability of the electrochemical sensor (AM194 sensor) consisting of AM194-MIP layer integrated with the electrode to selectively rebind AM194-MIP by measuring the electrochemical responses in the relevant solutions containing AM194. Furthermore, the ability of the sensor to discriminate between AM194 and similar peptides. Computational modelling using molecular docking method can be used to select an appropriate functional monomer for AM194-MIP formation. Cyclic voltammetry (CV) and differential pulse voltammetry (DPV) techniques can be used for the following characterization of the AM194-MIP preparation stages and for assessment of performance of the resulting AM194 sensor in terms of its capability to recognize selectively the target against interfering peptides.

2. Experimental part

2.1 Chemicals and materials

Sodium chloride (NaCl), disodium hydrogen phosphate, 4-aminothiophenol (4-ATP), 2-mercaptoethanol (2-ME), m-phenylenediamine (mPD) and acetic acid (AA) were purchased from Sigma-Aldrich. Dopamine (DA) was purchased from Honeywell Fluka. 3,3'-dithiobis[sulfosuccinimidylpropionate] (DTSSP) was purchased from Thermo Fisher Scientific Inc. Sulfuric acid, hydrogen peroxide, and potassium chloride were purchased from Lach-ner, S.R.O. Peptides QAKTFLDKFNHEAEDLFYQ (AM194), YFLDAEHNFK (AM174), YWDKIKDIGG (AM160) and LRRASLG (EV233) were received from Institute of Chemistry at Tartu University. All chemicals were of analytical grade or higher and were used as received without any further purification. All solutions were prepared in ultrapure water (resistivity 18.2 MΩ cm at 25 °C, EMD Millipore) and in phosphate buffered saline (PBS) with pH 7.4 (Na_2HPO_4 10 mM, KH_2PO_4 1.8 mM, NaCl 137 mM, KCl 2.7 mM) solution, chosen for its ability to replicate the osmolarity and ion concentrations found in the human body.

The glass plates coated with 200 nm of gold (Au plates) were used in this study as a working electrode and were purchased from Ssens bv of Netherlands.

2.2 Electrochemical measurements

Electrochemical measurements using such electrochemical techniques as cyclic voltammetry (CV) and differential pulse voltammetry (DPV) were made in an experimental electrochemical cell connected with Potentiostat/Galvanostat/ZRA "Reference 600" from Gamry Instruments. A conventional three-electrode system was used with an Au plate as a working electrode (WE) with working surface area equal to 0.56 cm^2, a platinum wire as a counter electrode (CE), and an $Ag/AgCl/KCl_{3M}$ as a reference electrode (RE) (Figure 12).

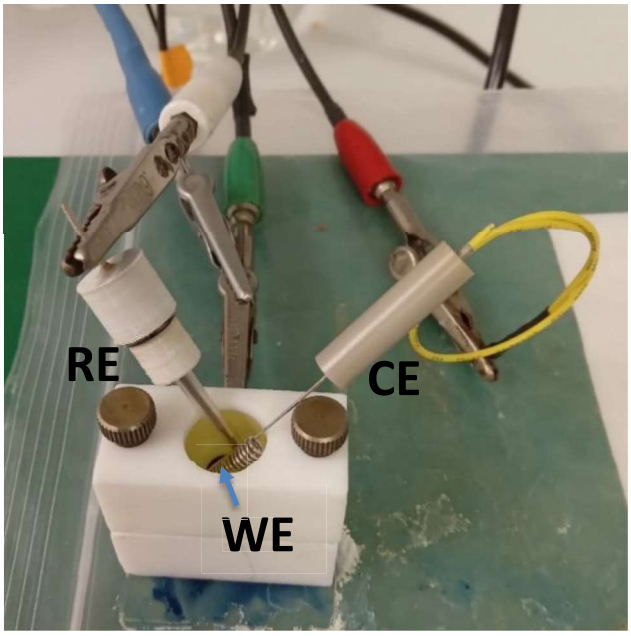

Figure 12. The experimental electrochemical cell with connected three-electrode system with Au plate inside the cell as working electrode (WE), $Ag/AgCl/KCl_{3M}$ as reference electrode (RE) and platinum wire as counter electrode (CE).

2.2.1 Cyclic voltammetry

CV measurements were carried out in a 0.3 M KCl solution containing 4 mM redox probe$K_3[Fe(CN)_6]/K_4[Fe(CN)_6]$. The potentials varied between -0.1 and 0.6 V at a scan rate of 50 mV/s with step size 2 mV. Five potential scan cycles were applied for each step.

2.2.2 Differential pulse voltammetry

DPV measurements have been performed in a 0.3 M KCl solution containing 4 mM redox probe $K_3[Fe(CN)_6]/K_4[Fe(CN)_6]$. DPV readings were done in the potential window between 0.05 and 0.5 V with a pulse amplitude of 25 mV, a pulse width of 0.05 s, a step potential of 2 mV, and a sample time of 0.1 s.

2.3 Functional monomer selection

Functional monomer for the preparation of AM194-MIP film with optimal performance was selected based on the prediction of binding energy potential between the monomer and AM194 using computational modelling. Several electropolymerizable monomers containing complementary functional groups were selected as candidate monomers. These include dopamine (DA), 3-aminophenylboronic acid (APBA), 3,4-ethylenedioxythiophene (EDOT) and m-phenylenediamine (mPD).

2.3.1 Molecular docking of AM194

Molecular docking procedures with Autodock 4.2.6 (from the Scripps Research Institute) were applied to selected center atoms and whole peptide rigid grid boxes. Three-dimensional (3D) X-ray crystal structure of the AM194 was adopted from Protein Data Bank (PDB) (ID: 7ZDQ). The candidate monomers were scored into the peptide as flexible ligands. The monomers and the peptide were first converted to Autodock tools format (into .pdbqt files) and the initial files for grid-box (.gpf) along with the docking procedure (.dpf) were prepared with Autodock tools and processed with Autodock 4.2.6 software.

2.4 Synthesis of AM194-MIP

The electrochemical surface imprinting approach previously developed by Syritski's group for protein-MIP preparation[129] was adapted in this study for AM194-MIP synthesis on the WE surface of the Au plate. The synthesis includes the following stages (Figure 13): (A) functionalization of the sensor surface with 4-ATP, then (B) with DTSSP crosslinker and (C) finally immobilization of the AM194 peptide with crosslinker; (D) electropolymerization of functional monomer to form a thin layer of polymer film around AM194 peptide molecule; (E) reduction of disulfide bond of DTSSP and (F) removal of the AM194 from the polymer matrix to form AM194-MIP film. AM194 covalent immobilization, polymer synthesis and peptide washing out process were characterized electrochemically by CV and DPV.

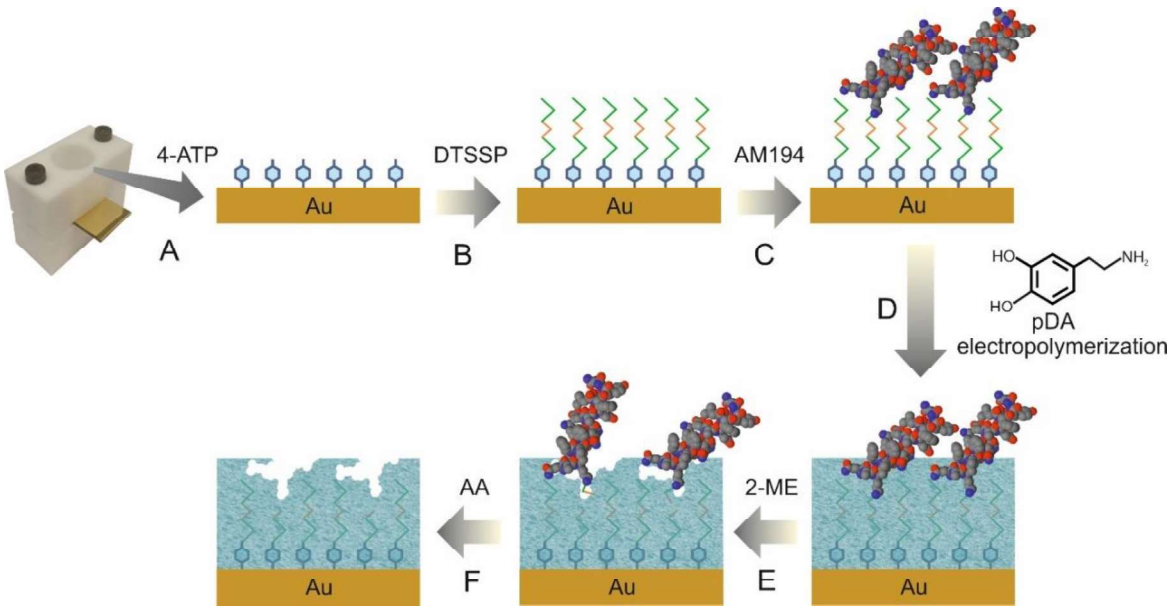

Figure 13. A scheme of sensor surface modification with the MIP. (A) assembling a 4-ATP functional monolayer; (B) attachment of DTSSP cleavable crosslinker; (C) AM194 covalent immobilization; (D) electropolymerization of DA; (E) cleavage of S-S bond of DTSSP with 2-ME; (F) washing out the AM194 molecules with AA.

2.4.1 Functionalization and immobilization

For AM194-MIP synthesis the Au plate was placed in the Ozone cleaner (Novascan, PSD Pro Series Digital UV Ozone System) for 1.5 hours and then rinsed abundantly with ultrapure water. Then the working surface of the Au plate was additionally cleaned electrochemically in 0.1 M H_2SO_4 solution, cycling the potential from 0 to 1.15 V at a scan rate of 100 mV/s for 5 cycles. Next, WE surface modification with 4-ATP was carried out by immersing the cleaned electrode in an ethanolic solution of 0.1 M 4-ATP for a duration of 30 minutes to form the self-assembled functional monolayer followed by thorough rinsing with ethanol to remove the unreacted 4-ATP molecules. After that the electrode was rinsed with ultrapure water and dried under a nitrogen flow. Afterwards, the 4-ATP-modified gold plate was functionalized by the cleavable linker by immersing in a 10 mM solution of DTSSP in PBS for approximately 30 minutes and followed by washing in ultrapure water. Finally, a 221 ng/mL solution of AM194 in PBS was applied to the ATP-DTSSP-modified Au plate for approximately 30 minutes to immobilize AM194 molecules.

2.4.2 Electrodeposition of poly-DA

The synthesis of poly-DA (pDA) on peptide-modified Au plates was performed in the experimental electrochemical cell connected with the electrochemical workstation (REF600-04077, Reference 600, Gamry Instruments, USA). The electrodeposition was carried out using galvanostatic synthesis method by applying a constant current for a certain amount of time on WE with surface area of 0.56 cm^2. These parameters can be used to find the applied charge density using Equation 2.1.

$$Q = \frac{I * t}{S}, \qquad \text{(Equation 2.1)}$$

where Q is the applied charge density, I is the current intensity of the polymerization, t is the polymerization time and S is the working surface area. Q have units in millicoulombs per square centimeter (mC/cm^2).

2.4.3 Peptide removal

Molecular imprints of AM194 in the polymer film were generated by washing out (WO) process by treating the polymer film with an ethanolic solution of 0.1M 2-mercaptoethanol (2-ME) for 15 minutes to cleave the S–S bond of DTSSP and facilitate the release of peptide, followed by washing with a 10% acetic acid (AA) solution for 15 minutes to dissociate non-covalent bonds between the polymer and the peptide.

A similar MIP preparation procedure was also adopted for the reference film, non-imprinted polymers (NIPs), although in this procedure there's no steps with peptide removal with 2-ME and AA.

2.5 Performance of AM194 sensor

In this study the electrochemical readout of the prepared AM194-MIP-based sensor (AM194 sensor) is founded on the indirect transduction and relied on the "gate effect", which occurs due to the occupancy of imprinted cavities within the MIP by analyte molecules (Section 1.2.1). The reversible redox pair $K_3[Fe(CN)_6]/K_4[Fe(CN)_6]$ was employed as a redox marker to monitor the indirect response of AM194 electrochemical sensors The sensor performance evaluation consisted of two main parts: a rebinding study and a selectivity study.

2.5.1 Rebinding study

The specific binding of the AM194 to the synthesized AM194-MIP film was analyzed using DPV technique in the presence of redox probe $K_3[Fe(CN)_6]/K_4[Fe(CN)_6]$ solution. The AM194-MIP-modified electrode incubated in PBS as blank solution for 15 minutes. Thereafter, a series of DPV measurements in a redox probe solution were carried out to obtain a stable baseline DPV response. Then, the sensor was incubated in the solution of varying concentrations of AM194 from 1 to 100 pg/ml in PBS solution. Since the concentration solutions were prepared in PBS, PBS was designated as the reference point, or zero-point concentration (0 pg/mL). Each incubation was done for a duration of 15 minutes. The recorded DPV current peaks values were used to acquire the AM194-MIP-based sensor normalized response signals (I_n).

$$I_n = \frac{I_0 - I}{I_0}, \qquad \text{(Equation 2.2)}$$

where I_0 is the peak value measured in the PBS blank solution and I is the peak value measured by DPV after rebinding at certain concentration. Both I_0 and I are recorded at the stable DPV peak current strengths and have units in microamperes (μA).

Furthermore, adsorption isotherms were generated to determine the adsorption capacity of AM194-MIP and -NIP towards AM194. Langmuir adsorption model, as depicted in Equation 2.3, was adopted to fit the binding isotherm and from that, both the dissociation constant (K_D) and maximum binding response at saturation (A_{sat}) values were obtained[130].

$$I_n = \frac{A_{sat} * C}{K_D + C}, \qquad \text{(Equation 2.3)}$$

where I_n and A_{sat} are sensor response signal after adsorption of the analyte on AM194-MIP and -NIP at the concentration C and its saturation value, respectively and K_D is equilibrium dissociation constant.

The imprinting factor (*IF*), that shows relation in binding towards the target analyte between prepared AM194-MIP and -NIP, was calculated from the equation below:

$$IF = \frac{A_{sat(MIP)}}{A_{sat(NIP)}}, \qquad \text{(Equation 2.4)}$$

where $A_{sat(MIP)}$ and $A_{sat(NIP)}$ are saturated response signals after AM194 adsorption on AM194-MIP and -NIP films, respectively.

2.5.2 Selectivity study

To determine the ability of the AM194-MIP to discriminate the AM194 from other similar molecules, a selectivity study was conducted. The normalized sensor responses (I_n) after rebinding the target peptide AM194 (Figure 14a) and other peptides at a concentration range of 1-100 pg/mL in PBS solution were compared the tested peptides included YFLDAEHNFK (AM174), YWDKIKDIGG (AM160) and LRRASLG (EV233) (Figure 14b, 14c and 14d). All peptide structures were drawn using the PepDraw website[131].

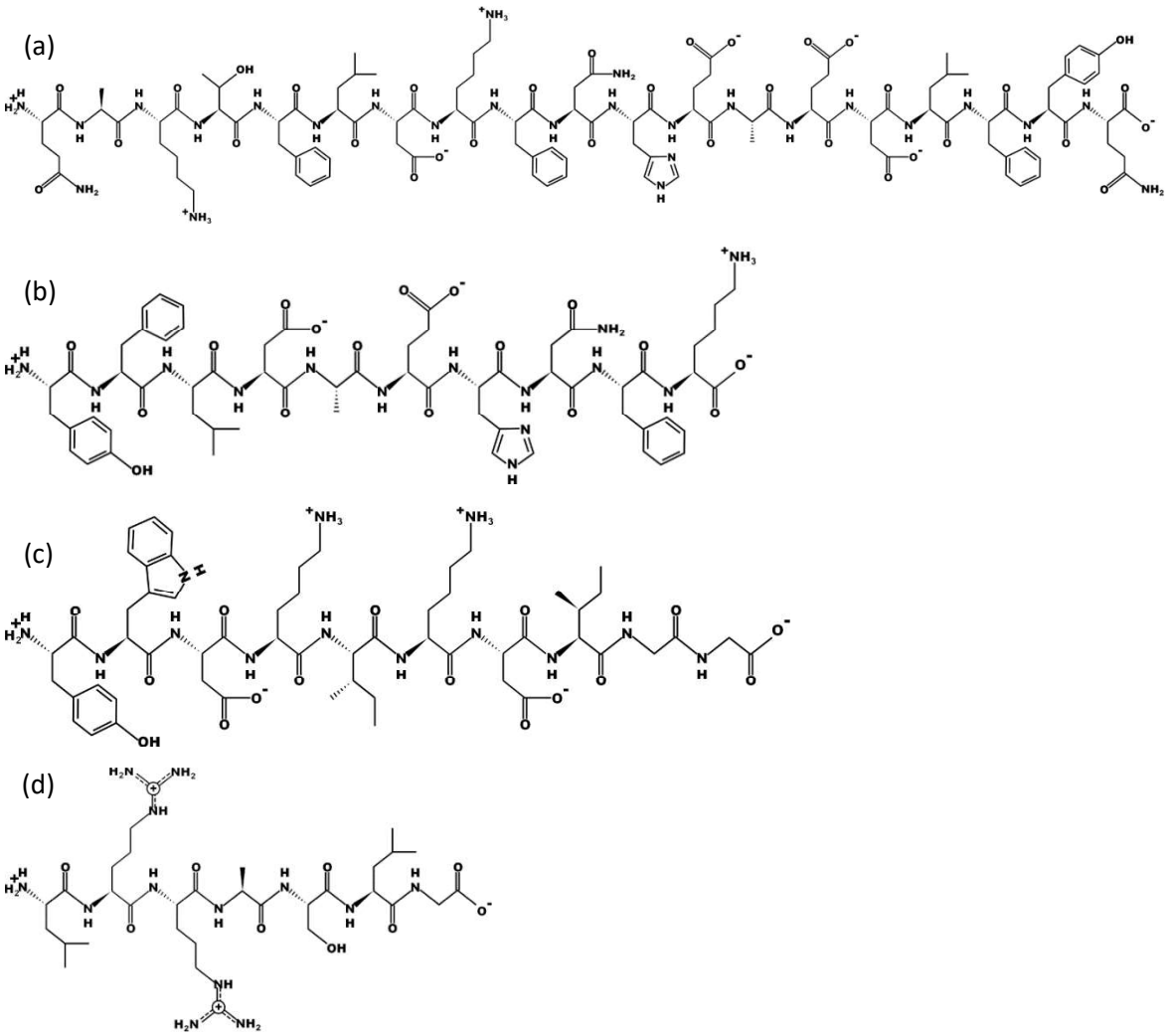

Figure 14. Primary structure of the peptide (a) QAKTFLDKFNHEAEDLFYQ (AM194), (b) YFLDAEHNFK (AM174), (c) YWDKIKDIGG (AM160) and (d) LRRASLG (EV233).

3. Results and discussion

3.1 Selection of functional monomer

A rational approach for selecting a functional monomer to synthesize AM194-MIP polymer was based on molecular docking. Molecular docking was performed to determine the binding energy of the binding positions between the AM194 and the functional monomer such as hydrogen bonds or electrostatic interactions. Computational tools and software can quantify the contribution of different types of non-covalent interactions to the total binding energy individually for the studied monomer-peptide complexes, but most often only the total binding energy is considered. Molecular docking goal is to predict the predominant binding sites of a ligand with any other molecule such as protein of known three-dimensional structure[132] and it has been applied for the rational selection of monomers for protein-MIPs[52]. The binding energy between the template and the functional monomer was assessed based on the calculated GScore value. GScore is an empirical scoring function which scores the energy-minimized poses of the monomers and approximates the monomer binding free energy, bearing in mind parameters such as Van der Waals interaction forces (*VdW*), electrostatic attractions (*Coul*), hydrogen bonds (*Hbond*), solvation effect (*Desolv*) and rotatable bonds energy (*Tors*), and GScore can be calculated using Equation 3.1[52,133].

$$\Delta\mathrm{GScore} = VdW + Coul + Hbond + Desolv + Tors, \quad \text{(Equation 3.1)}$$

For AM194-MIP formation, the monomer that produced the highest GScore energy in docked complex with AM194 was considered as the most suitable for experiments. According to the results obtained (Table 1), DA was seen to be the best monomer with the highest GScore value when compared with other functional monomers such as APBA, EDOT and mPD (Figure 15). Consequently, DA was selected as the polymer base for the AM194-MIP.

Table 1. Different functional monomers with their binding energy values with AM194.

Monomer	DA	APBA	EDOT	mPD
GScore, kcal/mol	4.91	3.92	3.58	3.27

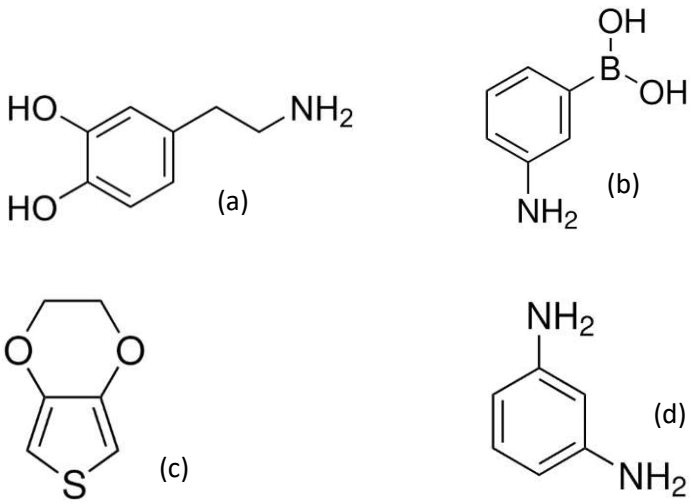

Figure 15. Chemical structures of (a) DA, (b) APBA, (c) EDOT and (d) mPD.

3.2 AM194-MIP preparation

3.2.1 Characterization of AM194-MIP preparation stages

The electrochemical surface imprinting approach previously developed by Syritski's group for protein-MIP preparation[129] was adapted in this study for AM194-MIP film synthesis. The synthesis included 3 main stages as represented in Figure 13: peptide immobilization via 4-ATP/DTSSP linker, polymer electrodeposition and peptide removal with WO process. The AM194-MIP synthesis strategy included at the first stage the covalent immobilization of the peptide at the electrode surface via the crosslinker DTSSP, which contains cleavable disulfide bond. The covalent bond is formed between the succinimide group of DTSSP and one of the lysine in amino acid sequence of AM194 as illustrated in Figure 16.

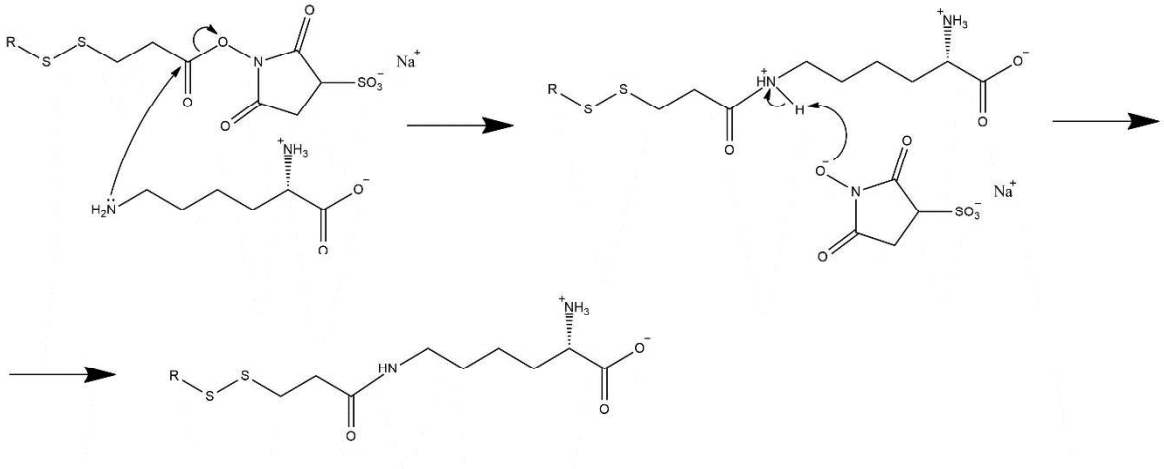

Figure 16. Covalent bond formation between one of the succinimide group of DTSSP and Lysine.

CV and DPV measurements were carried out to characterize the stages of WE modification step by step (Figure 17). As can be seen the redox peak current intensity decreased after each modification step, indicating hindered charge transfer at the electrode/solution interface due to the attachment of organic molecules. As observed in the CV and DPV plots, a huge decrease in peak current intensity occurred after the binding of DTSSP to the WE, which decline suggests successful binding of DTSSP to the functional monolayer. After immobilization of the AM194, the redox signal didn't decrease too much in relation to DTSSP, and this is quite expected because AM194 is not a super-massive protein, like the BDNF protein, which, when bound to DTSSP, greatly reduces the amount of faradaic current passed through the resulting cavities of the prepared MIP[134]. On the contrary, the AM194 is an extremely small template and does not cause a strong decrease in the electrochemical signal in a redox probe solution. After the subsequent electrodeposition of pDA, the peak current intensity was clearly reduced in both the CV and the DPV plots indicating hindered charge transfer at the electrode/solution interface due to formation of polymer from functional monomer. After the subsequent WO process the DPV current peak increase was observed due to the creation of the imprinted cavities (AM194 fingerprints) in the polymer.

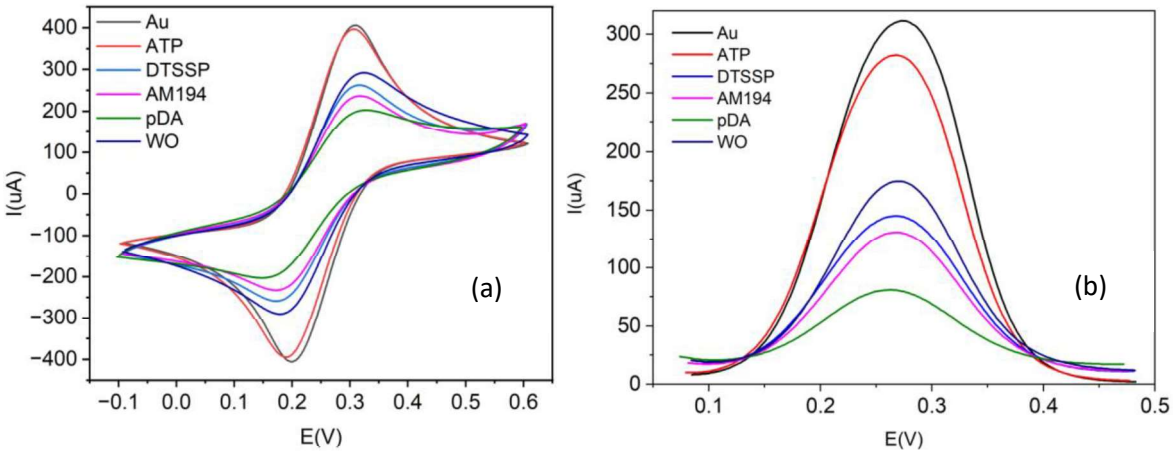

Figure 17. (a) CV and (b) DPV characterization of the stages for preparation of AM194-MIP. The stages include functionalization Au surface with 4-ATP, DTSSP, AM194, synthesis of pDA and finally WO process to form AM194-MIP. The CV and DPV measurements were performed in 0.3 M KCl solution containing 4 mM $K_3[Fe(CN)_6]/K_4[Fe(CN)_6]$.

3.2.2 Optimization of pDA electrochemical synthesis

The optimization aims to enhance the sensitivity of the AM194-MIP in detecting target through the imprints on the polymer film, thereby improving overall sensor performance.

Firstly, the concentration of monomer, DA, used for electrodeposition was varied. Three different AM194-MIPs and corresponding NIPs were prepared with pDA film electrodeposited at constant current of 500 µA applied during 5.6 s from PBS containing DA at concentrations of 2.5, 5, and 10 mM. The rebinding experiments were carried out at AM194 concentration range of 1-100 pg/mL and from the obtained binding isotherms (Appendix 1) saturated response values (A_{sat}) for each sensor were determined according to Equation 2.3 as well as the imprinting factor (IF) values according to Equation 2.4 (Figure 18 and Table 2).

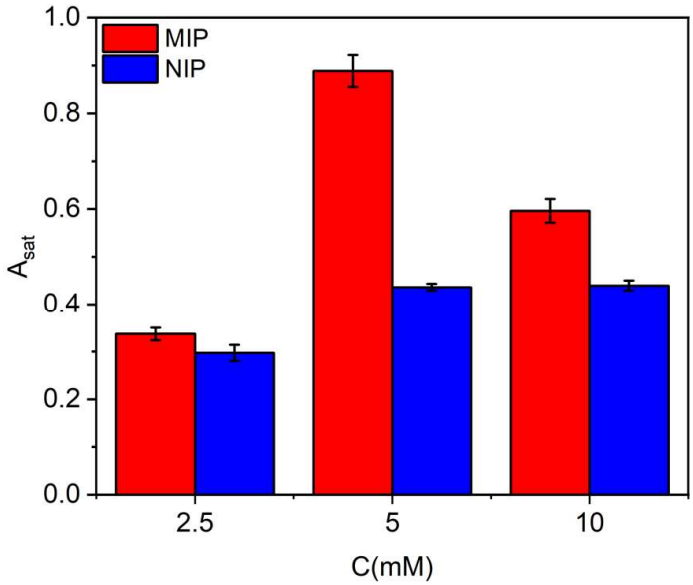

Figure 18. Saturated response values of the sensors modified with AM194-MIP and NIP films prepared by the electrodeposition of pDA from PBS containing different DA concentrations (2.5 mM, 5 mM, 10 mM) at constant current of 500 µA applied for 5.6 seconds.

Table 2. A_{sat} and IF values derived from fitting the AM194 adsorption r isotherms on pDA layer at a constant current of 500 µA applied for 5.6 s with different DA concentrations with Langmuir model.

	2.5 mM	5 mM	10 mM
A_{sat} AM194-MIP	0.34	0.89	0.60
A_{sat} AM194-NIP	0.30	0.44	0.44
IF	1.13	2.04	1.36

As can be seen the AM194-MIP exhibits the highest A_{sat} value when pDA electrodeposition was performed with DA concentration of 5 mM. Additionally, the highest IF value of 2.04 was attained under this condition, indicating that the AM194-MIP possesses two times higher binding capability towards the target peptide than corresponding NIP thus confirming the creation of selective binding sites (molecular imprints) during AM194-MIP preparation.

The next step involved optimization of the polymer thickness by adjusting the electrodeposition time. The deposition of a polymer with an appropriate thickness is critical to prevent the irreversible entrapment of a template and ensure its feasible removal during subsequent washing procedures[129]. By adjusting the time of the galvanostatic synthesis, the polymer film thickness can be easily controlled, providing possibility of customization the final MIP film thickness and efficiency[135]. To accomplish the polymerization time optimization, three different AM194-MIPs and corresponding NIPs were prepared, wherein pDA film was electrodeposited from PBS containing 5 mM of DA at constant current of 500 µA applied for various durations: 2.8, 5.6, and 8.4 seconds (Figure 19). These values were selected with intervals of 2.8 seconds, both lower and greater than 5.6 seconds, as used in the previous optimization step. Using Equation 2.1, these polymerization times of 2.8, 5.6, and 8.4 seconds can be converted into the applied charge density (Q) values of -2.5, 5 and 7.5 mC/cm^2, respectively. Then, the rebinding experiments were carried out at AM194 concentration range of 1-100 pg/mL and from the obtained binding isotherms (Appendix 2) saturated response values (A_{sat}) for each sensor were determined according to Equation 2.3 as well as the IF values according to Equation 2.4.

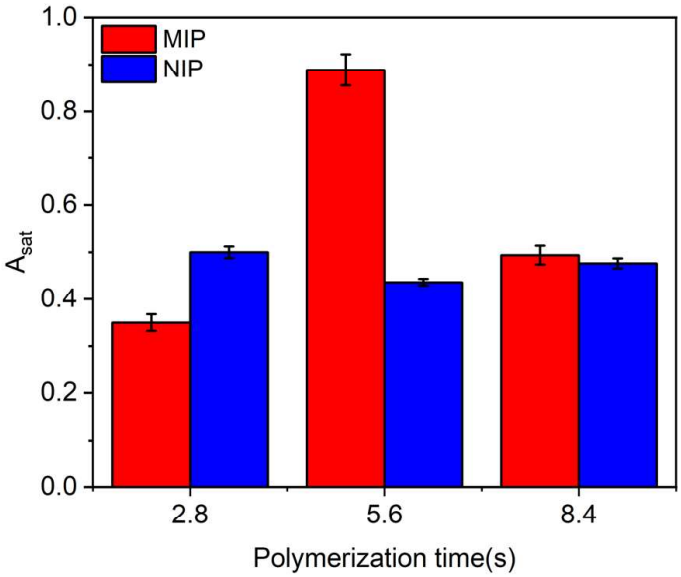

Figure 19. Saturated response values of the sensors modified with AM194-MIP and NIP films prepared by the electrodeposition of pDA from PBS containing 5 mM DA at a constant current of 500 µA applied for different time (2.8 s, 5.6 s, 8.4 s).

Table 3. A_{sat} and IF values derived from fitting the AM194 adsorption with Langmuir isotherm on pDA layer containing 5 mM DA for different polymerization time.

	2.8 s (2.5 mC/cm^2)	5.6 s (5 mC/cm^2)	8.4 s (7.5 mC/cm^2)
A_{sat} AM194-MIP	0.35	0.89	0.49
A_{sat} AM194-NIP	0.50	0.44	0.48
IF	0.70	2.04	1.04

The analysis of the results presented in Table 3 revealed that the A_{sat} and IF values for AM194-MIP prepared at the PDA electrodeposition conditions used during the monomer concentration optimization (5 mM of DA and 5.6 s), appeared the highest as compared with the AM194-MIP prepared at shorter or longer electrodeposition times. Consequently, the pDA film electrodeposition parameters such as 5mM DA in PBS and applied current of 500 µA for 5.6 s corresponding to charge density of 5 mC/cm^2 were determined as optimal and were used in further experiment for AM194 sensor preparation.

3.3 AM194 sensor performance study

The selective adsorption capability of the resulting AM194 sensor for the target analyte was assessed by measuring the DPV responses of the sensors modified with AM194-MIP and the corresponding NIP upon incubation in PBS containing varying concentrations of AM194 (1, 2, 5, 10, 25, 50, and 100 pg/mL). Figure 20a illustrates the consistent decrease in current peak with increasing concentration of AM194 in the case of AM194 sensor, indicating hindered charge transfer at the electrode/solution interface due to the MIP cavities blocking by the adsorbed analyte. Figure 20b depicts the DPV current peaks from the NIP sensor, that exhibits a less pronounced reduction in current peak with increasing analyte concentration compared to the AM194-MIP. Additionally, NIP sensor did not exhibit a significant concentration dependence. Table 4 represents the values of DPV peak current intensity and calculated normalized response signal (I_n) obtained from one of three independent measurements from three sensors.

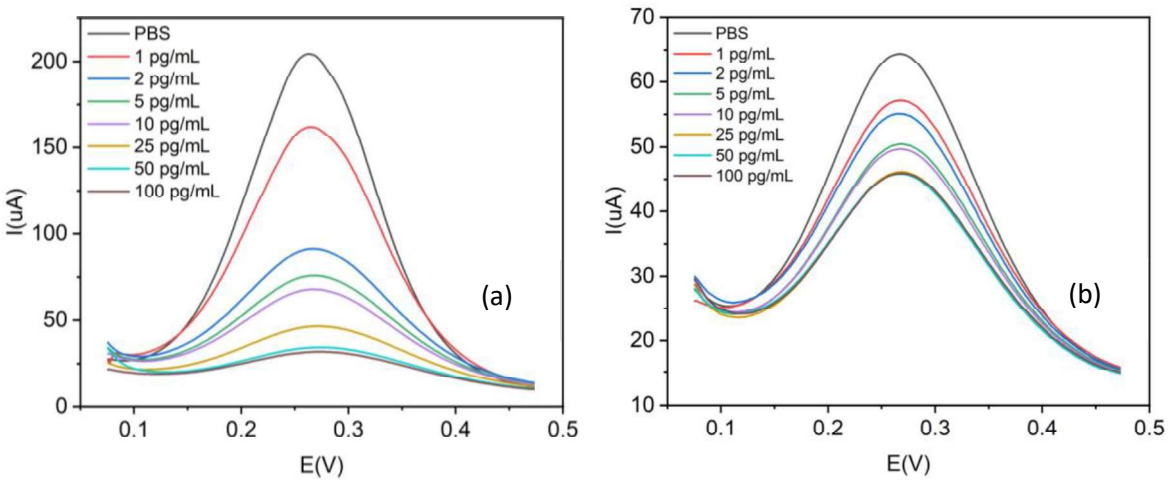

Figure 20. DPV signals of prepared sensors modified with (a) AM194-MIP and (b) AM194-NIP, obtained after incubation in different AM194 concentrations in PBS (1, 2, 5, 10, 25, 50 and 100 pg/mL).

Table 4. The values of DPV peak current intensity and calculated normalized response signals of AM194-MIP and AM194-NIP obtained in one of the rebinding experiments.

	AM194-MIP		AM194-NIP	
	I_{peak}, µA	I_n	I_{peak}, µA	I_n
PBS (0 pg/mL)	185.33	0	43.50	0
1 pg/mL	139.83	0.25	36.36	0.16
2 pg/mL	69.47	0.63	33.76	0.22
5 pg/mL	55.09	0.70	30.26	0.30
10 pg/mL	47.55	0.74	29.33	0.33
25 pg/mL	29.59	0.84	26.59	0.39
50 pg/mL	18.45	0.90	25.87	0.41
100 pg/mL	17.05	0.91	25.51	0.41

3.3.1 Binding isotherm analysis

AM194 adsorption isotherms were then constructed based on the analyte concentration and the calculated I_n values (Figure 21). These adsorption isotherms were fitted to the Langmuir model to determine the A_{sat} and the dissociation constant (K_D) values. The Langmuir adsorption isotherm method is employed in MIPs to describe the adsorption process of an analyte on a polymer surface. This method offers a straightforward approach to determine the amount of analyte adsorbed on a surface as a function of its concentration in solution. The model presumes that the surface is homogeneous, possessing a fixed number of equivalent binding sites that interact with the target analytes[136]. As observed, the AM194-MIP exhibits a much higher response to each AM194 concentration compared to the AM194-NIP for each of three independent measurements from three sensors. The coefficient of determination (R^2) was calculated, serving as a statistical measure, indicating the accuracy of the model's fit to the available data. All the obtained results for A_{sat}, K_D and R^2 values are presented in Table 5. The IF parameter was calculated as the ratio of saturated responses of MIP and NIP to AM194 (Equation 2.4), and it equaled 2.04. This value highlights the enhanced binding of AM194 peptide to AM194-MIP as compared to NIP, indicating that the binding sites were created within the pDA polymer prepared under optimized conditions and clearly made a significant contribution to the recognition of the oligopeptide AM194.

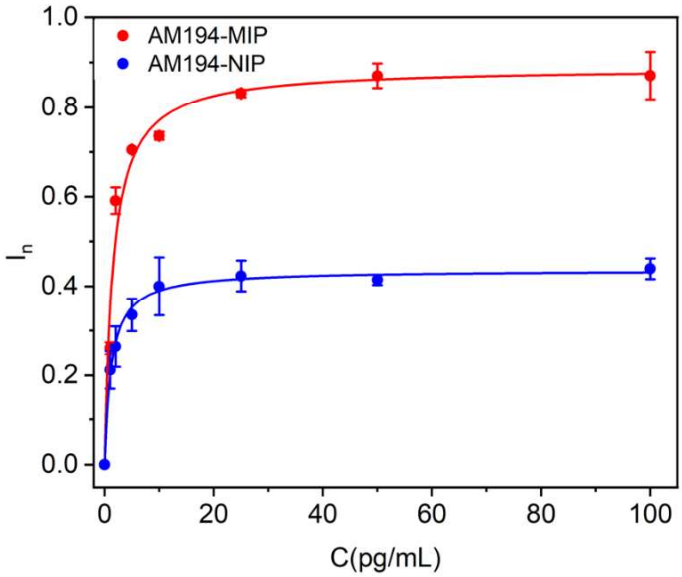

Figure 21. AM194 adsorption isotherm on the AM194-MIP (red) and AM194-NIP (blue), fitted with LF adsorption model.

Table 5. Parameters derived from fitting the AM194 adsorption isotherms (Figure 21) to Langmuir adsorption model.

	AM194-MIP	AM194-NIP
A_{sat} AM194	0.89 ± 0.03	0.44 ± 0.01
K_D, pg/mL	1.53 ± 0.30	1.20 ± 0.11
R^2	0.97	0.99
IF	2.04	

3.3.2 Sensitivity of AM194 sensor

To establish the analytical sensitivity of the AM194 sensor, a rebinding experiment was conducted using AM194 concentrations ranging from 50 to 500 fg/mL (50, 100, 250, 400, and 500 fg/mL), where the sensor demonstrated a pseudo-linear response towards against AM194. The normalized responses obtained from DPV plots (Figure 22a) were used to generate a linear regression fit (Figure 22b). Utilizing the parameters obtained from the linear regression analysis such as Slope and SD value (Table 6), values for the Limit of Detection (*LoD*) and Limit of Quantitation (*LoQ*) were calculated using Equation 3.2.

$$LoD = \frac{3.3 * SD}{\text{Slope}} \text{ and} \qquad \text{(Equation 3.2)}$$

$$LoQ = \frac{10 * SD}{\text{Slope}},$$

where *SD* is the standard deviation of linear regression and *Slope* is describing the direction and steepness of the regression line.

It was found that the AM194 sensor was capable of detecting AM194 in PBS with LoD of 24 fg/ml and LoQ of 72 fg/ml. The obtained LoD and LoQ values can be compared with other studies that used the MIP technology to detect peptides of different sizes and using different methods. Table 7 refers to some example studies, including the study in this thesis, that used MIP-based sensors and

shows which peptides were used, their sizes in amino acid length, their LoD and LoQ values, linear range responses, and what detection methods were used to achieve low detection levels.

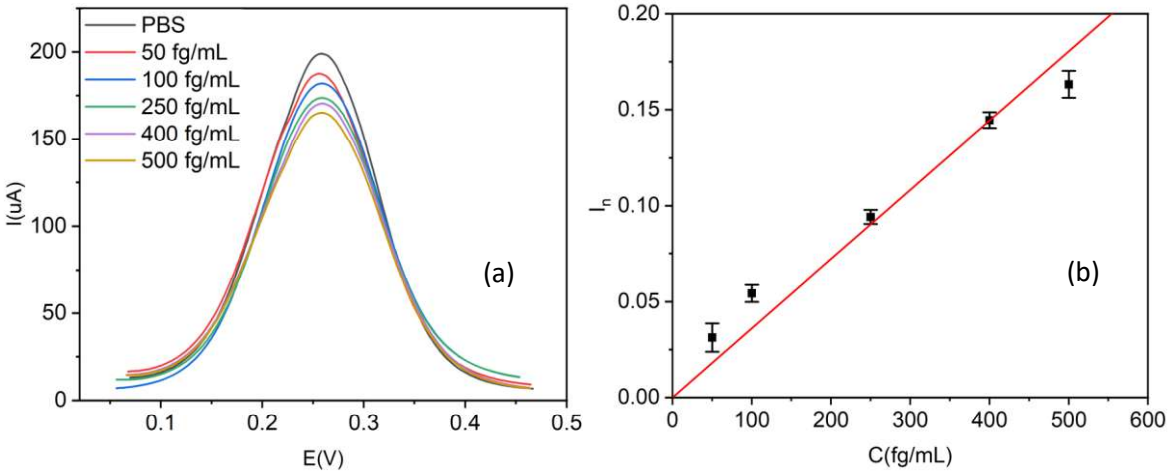

Figure 22. (a) DPV plot and (b) linear regression fit of AM194 sensor responses to low concentrations of AM194 (50, 100, 250, 400 and 500 fg/mL range) in PBS. The point and error bars represent mean and standard deviation of three measurements carried out by three independent AM194 sensors.

Table 6. Parameters derived from linear regression analysis of AM194 sensor responses to AM194 at concentration range of 50-500 fg/mL.

	AM194-MIP
Intercept	0
Slope	0.36 ± 0.02
SD	2.59
R^2	0.99

Table 7. Comparision of MIP-based sensors for peptide detection.

Study peptide	Peptide length	LoD	LoQ	Linear range	Detection method	Reference
EGFR	53 aa[137]	3 nM	-	0-500 nM	TD[a]	[104]
Carnosine	2 aa	55 µM	-	0.1-1 mM	EIS[b]	[105]
MEL	26 aa	0.3 µg/mL	1.1 µg/mL	1-30 µg/mL	QCM[c]	[106]
Insulin	51 aa[138]	1.9 pM	6.2 pM	20-70 pM	EDS[d]	[139]
BNP	17 aa	0.208 pg/mL	-	0.25-5000 pg/mL	FD[e]	[140]
AM194	19 aa	24 fg/mL	72 fg/mL	50-500 fg/mL	DPV	This study

[a]Thermal Detection, [b]Electrochemical Impedance Spectroscopy, [c]Quartz Crystal Microbalance, [d]Energy-Dispersive Spectroscopy, [e]Fluorescent Detection.

3.4 Selectivity study

To assess the selectivity of the prepared AM194-MIP, the responses of the sensor towards similar molecules, i.e. "interfering molecules" were measured. These molecules included the peptide

sequences such as YFLDAEHNFK (AM174), YWDKIKDIGG (AM160), and LRRASLG (EV233). AM174 possesses a central amino acid sequence almost similar to that of AM194 but in reverse order. AM160 was selected as a peptide with a different amino acid sequence but the same size as AM174. EV233 was selected due to its smaller size as compared to AM194, which could potentially fit into imprinted cavities of AM194-MIP.

For this experiment, the same concentration range of peptides in PBS solution were prepared (from 1 to 100 pg/mL). The results of these experiments revealed that the AM194-MIP exhibited higher responses to AM194 oligopeptide as compared to interfering peptides (Figure 23). Notably, at concentrations of 2 or 5 pg/mL, the sensor responses to AM194 were nearly six times higher than its responses to the structurally similar but smaller peptide, AM174. It is also worth mentioning that due to similarity in amino acid sequence the signals obtained upon AM174 binding were the highest among responses to other interfering peptides and demonstrated concentration dependence.

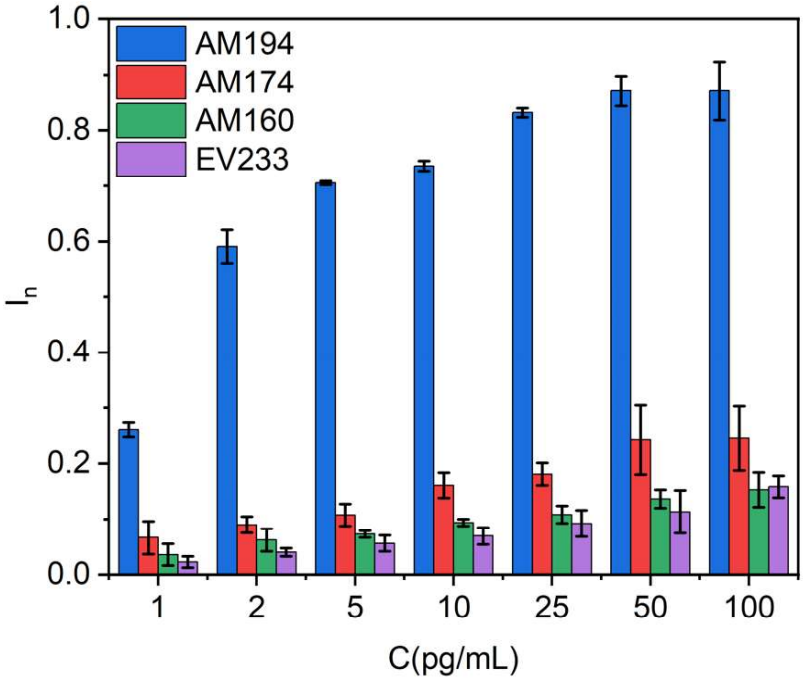

Figure 23. The responses of AM194 sensor to different peptides: AM194, AM174, AM160 and EV233 in concentration range 1-100 pg/mL in PBS.

4. Conclusions

This thesis presented the development of a peptide-selective electrochemical sensor based on the molecularly imprinted polymer (MIP) as a recognition element for detecting the ACE2 peptide fragment - QAKTFLDKFNHEAEDLFYQ (AM194). The AM194 with a sequence of 19 amino acids, selected as a model target peptide, was molecularly imprinted for the first time using electrochemical surface imprinting approach. The electrochemical techniques such as Cyclic Voltammetry (CV) and Differential Pulse Voltammetry (DPV) were utilized to characterize each stage of AM194-MIP formation as well as to measure the responses of the resulted AM194 sensor towards the target and interfering analytes. The following conclusions can be drawn from this work:

- Dopamine (DA) was found to be a more appropriate functional monomer for building the AM194-MIP based on the molecular docking results as demonstrated the highest GScore value for the AM194 and DA complex versus complexes formed with APBA, EDOT and mPD.
- Polydopamine (pDA) film electrodeposited galvanostatically employing current of 500 µA for 5.6 s delivering 5 mC/cm^2 to the working electrode in 5 mM DA diluted in PBS resulted in a polymer film, which after the template removal treatment turned into AM194-MIP possessing the higher binding capability to AM194. These parameters were determined as optimal for AM194-MIP layer for following testing of AM194 sensor.
- The Langmuir adsorption model was suitable to describe the adsorption of AM194 on AM194-MIP. The IF value of 2.04, calculated from the ratio of the saturated binding of AM194 on AM194-MIP and NIP, indicated an enhanced binding capability of AM194-MIP compared to NIP. This suggests the possible formation of AM194-selective binding sites in AM194-MIP under optimized conditions.
- AM194 sensor, representing the AM194-MIP layer attached to the electrode and signaling towards AM194 via changes in DPV current intensity, showed capability to detect AM194 with LoD of 24 fg/ml and LoQ of 72 fg/ml in PBS solution. This exceeds the LoD and LoQ values for peptide detection by the other reported MIP sensors.
- AM194 sensor showed selectivity towards the target peptide, AM194, as demonstrated by comparison of its responses towards the other similar peptides such as AM174, AM160 and EV233.

Ultimately, this thesis demonstrates the fabrication of a MIP-based electrochemical sensor capable of selectively detecting AM194, thereby achieving the main goals of this work. In future, more complex solutions can be used for AM194 testing, e.g. simulating biological fluids or real biological fluids such serum or plasma. This will require the improvement of analytical performance of the sensor by further optimization of MIP synthesis and measurement parameters. The results obtained in the course of this work lay the groundwork for future research in the development of peptide MIP-based sensors, which will significantly contribute to the development of cost-effective and rapid analytical tools for clinical diagnostics and environmental monitoring.

Acknowledgments

First, I want to extend my deep gratitude to my supervisors **Dr. Vitali Syritski** and **Dr. Jekaterina Reut**, for their invaluable guidance, support, and assistance throughout the course of my thesis. I am especially grateful for their supervision, help in writing, and analysis of the results. Their patience and timely advice were necessary in the completion of this thesis. I also appreciate their consideration of my comments, thoughts, and ideas, which contributed to the advancement of this study.

Additionally, I would like to thank **Dr. Roman Borozнjak** for his valuable assistance during the practical part of the thesis, including his advices and support in organizing and compiling important data.

I am also grateful to **Vu Bao Chau Nguyen** for his readiness to help, pleasant communication, and helpful advice on topics related to this work.

Finally, I want to express my heartfelt appreciation to my **fiancée**, who provided unwavering support both physically and mentally throughout this study. I am also thankful to my **family**, **loved ones**, and **friends** for their encouragement and belief in me.

This work was supported by the **Estonian Research Council grants** (**PRG307** and **PRG2113**). Also, I thank the **Institute of Chemistry at Tartu University** and **Dr. Aleksei Kuznetsov** for providing the necessary peptide sequences.

References

(1) Sreekumar, G.; Parashar, A.; Somanathan, S.; Mishra, S.; Singh, A.; Sheikh, I.; Sravani, D. Overview of Biosensors and Their Application: A Review. *Eur. Chem. Bull.* **2023**, 3247–3255. https://doi.org/10.31838/ecb/2023.12.Si9.293.

(2) Baranwal, J.; Barse, B.; Gatto, G.; Broncova, G.; Kumar, A. Electrochemical Sensors and Their Applications: A Review. *Chemosensors* **2022**, *10* (9), 363. https://doi.org/10.3390/chemosensors10090363.

(3) BelBruno, J. J. Molecularly Imprinted Polymers. *Chem. Rev.* **2019**, *119* (1), 94–119. https://doi.org/10.1021/acs.chemrev.8b00171.

(4) Nguyen, V. B. C.; Ayankojo, A. G.; Reut, J.; Rappich, J.; Furchner, A.; Hinrichs, K.; Syritski, V. Molecularly Imprinted Co-Polymer for Class-Selective Electrochemical Detection of Macrolide Antibiotics in Aqueous Media. *Sens. Actuators B Chem.* **2023**, *374*, 132768. https://doi.org/10.1016/j.snb.2022.132768.

(5) Raziq, A.; Kidakova, A.; Boroznjak, R.; Reut, J.; Öpik, A.; Syritski, V. Development of a Portable MIP-Based Electrochemical Sensor for Detection of SARS-CoV-2 Antigen. *Biosens. Bioelectron.* **2021**, *178*, 113029. https://doi.org/10.1016/j.bios.2021.113029.

(6) Ayankojo, A. G.; Reut, J.; Ciocan, V.; Öpik, A.; Syritski, V. Molecularly Imprinted Polymer-Based Sensor for Electrochemical Detection of Erythromycin. *Talanta* **2020**, *209*, 120502. https://doi.org/10.1016/j.talanta.2019.120502.

(7) Bielka, H.; Sharon, N.; Webb, E. C.; Karlson, P. NOMENCLATURE AND SYMBOLISM FORAMINO ACIDS AND PEPTIDES. **1984**.

(8) Ian W. Hamley. *Introduction to Peptide Science | Wiley*. Wiley.com. https://www.wiley.com/en-us/Introduction+to+Peptide+Science-p-9781119698173 (accessed 2024-03-26).

(9) Wang, L.; Wang, N.; Zhang, W.; Cheng, X.; Yan, Z.; Shao, G.; Wang, X.; Wang, R.; Fu, C. Therapeutic Peptides: Current Applications and Future Directions. *Signal Transduct. Target. Ther.* **2022**, *7*, 48. https://doi.org/10.1038/s41392-022-00904-4.

(10) Mahendru, S.; Roy, K.; Kukreti, S. Peptide Biomarkers: Exploring the Diagnostic Aspect. *Curr. Protein Pept. Sci. 18* (9), 914–919.

(11) Canfarotta, F.; Lezina, L.; Guerreiro, A.; Czulak, J.; Petukhov, A.; Daks, A.; Smolinska-Kempisty, K.; Poma, A.; Piletsky, S.; Barlev, N. A. Specific Drug Delivery to Cancer Cells with Double-Imprinted Nanoparticles against Epidermal Growth Factor Receptor. *Nano Lett.* **2018**, *18* (8), 4641–4646. https://doi.org/10.1021/acs.nanolett.7b03206.

(12) Chen, W.; Meng, Z.; Xue, M.; Shea, K. J. Molecular Imprinted Photonic Crystal for Sensing of Biomolecules. *Mol. Imprinting* **2016**, *4* (1), 1–12. https://doi.org/10.1515/molim-2016-0001.

(13) Bossi, A. M.; Sharma, P. S.; Montana, L.; Zoccatelli, G.; Laub, O.; Levi, R. Fingerprint-Imprinted Polymer: Rational Selection of Peptide Epitope Templates for the Determination of Proteins by Molecularly Imprinted Polymers. *Anal. Chem.* **2012**, *84* (9), 4036–4041. https://doi.org/10.1021/ac203422r.

(14) Wang, Y.; Xu, H.; Zhang, J.; Li, G. Electrochemical Sensors for Clinic Analysis. *Sensors* **2008**, *8* (4), 2043–2081. https://doi.org/10.3390/s8042043.

(15) Kempahanumakkagari, S.; Vellingiri, K.; Deep, A.; Kwon, E. E.; Bolan, N.; Kim, K.-H. Metal–Organic Framework Composites as Electrocatalysts for Electrochemical Sensing Applications. *Coord. Chem. Rev.* **2018**, *357*, 105–129. https://doi.org/10.1016/j.ccr.2017.11.028.

(16) Woellner, M.; Hausdorf, S.; Klein, N.; Mueller, P.; Smith, M. W.; Kaskel, S. Adsorption and Detection of Hazardous Trace Gases by Metal–Organic Frameworks. *Adv. Mater.* **2018**, *30* (37), 1704679. https://doi.org/10.1002/adma.201704679.

(17) Wang, P.-L.; Xie, L.-H.; Joseph, E. A.; Li, J.-R.; Su, X.-O.; Zhou, H.-C. Metal–Organic Frameworks for Food Safety. *Chem. Rev.* **2019**, *119* (18), 10638–10690. https://doi.org/10.1021/acs.chemrev.9b00257.

(18) Hulanicki, A.; Glab, S.; Ingman, F. Chemical Sensors: Definitions and Classification. *Pure Appl. Chem.* **1991**, *63* (9), 1247–1250. https://doi.org/10.1351/pac199163091247.

(19) Morales, M. A.; Mark Halpern, J. Guide to Selecting a Biorecognition Element for Biosensors. *Bioconjug. Chem.* **2018**, *29* (10), 3231–3239. https://doi.org/10.1021/acs.bioconjchem.8b00592.

(20) Thévenot, D. R.; Toth, K.; Durst, R. A.; Wilson, G. S. Electrochemical Biosensors: Recommended Definitions and Classification1. *Biosens. Bioelectron.* **2001**, *16* (1), 121–131. https://doi.org/10.1016/S0956-5663(01)00115-4.

(21) WatElectronics. *Biosensor : Types, Interfacing, Characteristics & Its Applications*. WatElectronics.com. https://www.watelectronics.com/biosensor/ (accessed 2024-03-26).

(22) Mehrotra, P. Biosensors and Their Applications – A Review. *J. Oral Biol. Craniofacial Res.* **2016**, *6* (2), 153–159. https://doi.org/10.1016/j.jobcr.2015.12.002.

(23) Wells, P. K.; Smutok, O.; Guo, Z.; Alexandrov, K.; Katz, E. Fluorometric Biosensing of α-Amylase Using an Artificial Allosteric Biosensor Immobilized on Nanostructured Interface. *Talanta* **2023**, *255*, 124215. https://doi.org/10.1016/j.talanta.2022.124215.

(24) Jandas, P. J.; Luo, J.; Quan, A.; Qiu, C.; Cao, W.; Fu, C.; Fu, Y. Q. Highly Selective and Label-Free Love-Mode Surface Acoustic Wave Biosensor for Carcinoembryonic Antigen Detection Using a Self-Assembled Monolayer Bioreceptor. *Appl. Surf. Sci.* **2020**, *518*, 146061. https://doi.org/10.1016/j.apsusc.2020.146061.

(25) Jalalvand, A. R. A Novel Amperometric Biosensor for Multi-Enzymatic Biosensing of Triglycerides. *Sens. Int.* **2023**, *4*, 100206. https://doi.org/10.1016/j.sintl.2022.100206.

(26) Fatoyinbo, H. O.; Hughes, M. P. Biosensors. In *Encyclopedia of Nanotechnology*; Bhushan, B., Ed.; Springer Netherlands: Dordrecht, 2012; pp 329–345. https://doi.org/10.1007/978-90-481-9751-4_129.

(27) Grieshaber, D.; MacKenzie, R.; Vörös, J.; Reimhult, E. Electrochemical Biosensors - Sensor Principles and Architectures. *Sensors* **2008**, *8* (3), 1400–1458. https://doi.org/10.3390/s80314000.

(28) Singh, A. K.; Mittal, S.; Das, M.; Saharia, A.; Tiwari, M. Optical Biosensors: A Decade in Review. *Alex. Eng. J.* **2023**, *67*, 673–691. https://doi.org/10.1016/j.aej.2022.12.040.

(29) Pohanka, M. The Piezoelectric Biosensors: Principles and Applications, a Review. *Int. J. Electrochem. Sci.* **2017**, *12* (1), 496–506. https://doi.org/10.20964/2017.01.44.

(30) Ramanathan, K.; Rank, M.; Svitel, J.; Dzgoev, A.; Danielsson, B. The Development and Applications of Thermal Biosensors for Bioprocess Monitoring. *Trends Biotechnol.* **1999**, *17* (12), 499–505. https://doi.org/10.1016/S0167-7799(99)01378-5.

(31) Biosensor Recognition Elements. *Curr. Issues Mol. Biol.* **2008**. https://doi.org/10.21775/cimb.010.001.

(32) Lucarelli, F.; Marrazza, G.; Turner, A. P. F.; Mascini, M. Carbon and Gold Electrodes as Electrochemical Transducers for DNA Hybridisation Sensors. *Biosens. Bioelectron.* **2004**, *19* (6), 515–530. https://doi.org/10.1016/S0956-5663(03)00256-2.

(33) Ronkainen, N. J.; Halsall, H. B.; Heineman, W. R. Electrochemical Biosensors. *Chem. Soc. Rev.* **2010**, *39* (5), 1747–1763. https://doi.org/10.1039/B714449K.

(34) *Electrodes and Accessories*. https://www.als-japan.com/1829.html (accessed 2024-04-09).

(35) Quesada-González, D.; Merkoçi, A. Nanomaterial-Based Devices for Point-of-Care Diagnostic Applications. *Chem. Soc. Rev.* **2018**, *47* (13), 4697–4709. https://doi.org/10.1039/C7CS00837F.

(36) Renedo, O. D.; Alonso-Lomillo, M. A.; Martínez, M. J. A. Recent Developments in the Field of Screen-Printed Electrodes and Their Related Applications. *Talanta* **2007**, *73* (2), 202–219. https://doi.org/10.1016/j.talanta.2007.03.050.

(37) Yu, M.; Feng, X. Thin-Film Electrode-Based Supercapacitors. *Joule* **2019**, *3* (2), 338–360. https://doi.org/10.1016/j.joule.2018.12.012.

(38) *Graphene modified Screen-Printed Carbon Electrode | Metrohm*. https://www.metrohm.com/en/products/1/10gp/110gph.html (accessed 2024-04-10).

(39) *Thin-film Electrochemical Sensors | MicruX*. https://www.micruxfluidic.com/en/electrochemical-solutions/thin-film-electrochemical-sensors/ (accessed 2024-04-10).

(40) Scholarly Community Encyclopedia. *Types of Electrochemical Sensors*. https://encyclopedia.pub/entry/33545 (accessed 2024-04-09).

(41) Stradiotto, N. R.; Yamanaka, H.; Zanoni, M. V. B. Electrochemical Sensors: A Powerful Tool in Analytical Chemistry. *J. Braz. Chem. Soc.* **2003**, *14*, 159–173. https://doi.org/10.1590/S0103-50532003000200003.

(42) Moro, G.; De Wael, K.; Moretto, L. M. Challenges in the Electrochemical (Bio)Sensing of Nonelectroactive Food and Environmental Contaminants. *Curr. Opin. Electrochem.* **2019**, *16*, 57–65. https://doi.org/10.1016/j.coelec.2019.04.019.

(43) Iskierko, Z.; Sharma, P. S.; Bartold, K.; Pietrzyk-Le, A.; Noworyta, K.; Kutner, W. Molecularly Imprinted Polymers for Separating and Sensing of Macromolecular Compounds and Microorganisms. *Biotechnol. Adv.* **2016**, *34* (1), 30–46. https://doi.org/10.1016/j.biotechadv.2015.12.002.

(44) Liu, G. Grand Challenges in Biosensors and Biomolecular Electronics. *Front. Bioeng. Biotechnol.* **2021**, *9*, 707615. https://doi.org/10.3389/fbioe.2021.707615.

(45) Vigneshvar, S.; Sudhakumari, C. C.; Senthilkumaran, B.; Prakash, H. Recent Advances in Biosensor Technology for Potential Applications - An Overview. *Front. Bioeng. Biotechnol.* **2016**, *4*, 11. https://doi.org/10.3389/fbioe.2016.00011.

(46) Varshney, M.; Mallikarjunan, K. Challenges in Biosensor Development: Detection Limit, Detection Time, and Specificity. *Resour. Eng. Technol. Sustain. World* **2009**, *16* (7), 18–21.

(47) Ayankojo, A. G.; Boroznjak, R.; Reut, J.; Tuvikene, J.; Timmusk, T.; Syritski, V. Electrochemical Sensor Based on Molecularly Imprinted Polymer for Rapid Quantitative Detection of Brain-Derived Neurotrophic Factor. *Sens. Actuators B Chem.* **2023**, *397*, 134656. https://doi.org/10.1016/j.snb.2023.134656.

(48) Buensuceso, C. E.; Tiu, B. D. B.; Lee, L. P.; Sabido, P. M. G.; Nuesca, G. M.; Caldona, E. B.; del Mundo, F. R.; Advincula, R. C. Electropolymerized-Molecularly Imprinted Polymers (E-MIPS) as Sensing Elements for the Detection of Dengue Infection. *Anal. Bioanal. Chem.* **2022**, *414* (3), 1347–1357. https://doi.org/10.1007/s00216-021-03757-y.

(49) Haupt, K.; Medina Rangel, P. X.; Bui, B. T. S. Molecularly Imprinted Polymers: Antibody Mimics for Bioimaging and Therapy. *Chem. Rev.* **2020**, *120* (17), 9554–9582. https://doi.org/10.1021/acs.chemrev.0c00428.

(50) Valkova, P.; Pohanka, M. Novel Trends in Electrochemical Biosensors for Early Diagnosis of Alzheimer's Disease. *Int. J. Anal. Chem.* **2021**, *2021*, e9984876. https://doi.org/10.1155/2021/9984876.

(51) Pilvenyte, G.; Ratautaite, V.; Boguzaite, R.; Samukaite-Bubniene, U.; Plausinaitis, D.; Ramanaviciene, A.; Bechelany, M.; Ramanavicius, A. Molecularly Imprinted Polymers for the Recognition of Biomarkers of Certain Neurodegenerative Diseases. *J. Pharm. Biomed. Anal.* **2023**, *228*, 115343. https://doi.org/10.1016/j.jpba.2023.115343.

(52) Boroznjak, R. *A Computational Approach for Rational Monomer Selection in Molecularly Imprinted Polymer Synthesis: = Monomeeride Valiku Protsessi Modelleerimine Optimaalse Monomeeri Leidmiseks Molekulaarselt Jäljendatud Polümeeride Sünteesil*; Thesis on natural and exact sciences; TUT Press: Tallinn, 2017.

(53) Li, Y.; Luo, L.; Kong, Y.; Li, Y.; Wang, Q.; Wang, M.; Li, Y.; Davenport, A.; Li, B. Recent Advances in Molecularly Imprinted Polymer-Based Electrochemical Sensors. *Biosens. Bioelectron.* **2024**, *249*, 116018. https://doi.org/10.1016/j.bios.2024.116018.

(54) Couto, R. A. S.; Costa, S. S.; Mounssef, B.; Pacheco, J. G.; Fernandes, E.; Carvalho, F.; Rodrigues, C. M. P.; Delerue-Matos, C.; Braga, A. A. C.; Moreira Gonçalves, L.; Quinaz, M. B. Electrochemical Sensing of Ecstasy with Electropolymerized Molecularly Imprinted Poly(*o*-Phenylenediamine) Polymer on the Surface of Disposable Screen-Printed Carbon Electrodes. *Sens. Actuators B Chem.* **2019**, *290*, 378–386. https://doi.org/10.1016/j.snb.2019.03.138.

(55) Yoshimi, Y.; Sato, K.; Ohshima, M.; Piletska, E. Application of the 'Gate Effect' of a Molecularly Imprinted Polymer Grafted on an Electrode for the Real-Time Sensing of Heparin in Blood. *Analyst* **2013**, *138* (17), 5121–5128. https://doi.org/10.1039/C3AN00909B.

(56) Ayankojo, A. G.; Boroznjak, R.; Reut, J.; Öpik, A.; Syritski, V. Molecularly Imprinted Polymer Based Electrochemical Sensor for Quantitative Detection of SARS-CoV-2 Spike Protein. *Sens. Actuators B Chem.* **2022**, *353*, 131160. https://doi.org/10.1016/j.snb.2021.131160.

(57) Allowances, N. R. C. (US) S. on the T. E. of the R. D. Protein and Amino Acids. In *Recommended Dietary Allowances: 10th Edition*; National Academies Press (US), 1989.

(58) Peptide Bond. *Wikipedia*; 2024.

(59) Guillier, F.; Orain, D.; Bradley, M. Linkers and Cleavage Strategies in Solid-Phase Organic Synthesis and Combinatorial Chemistry. *Chem. Rev.* **2000**, *100* (6), 2091–2158. https://doi.org/10.1021/cr980040+.

(60) Chan, W.; White, P. *Fmoc Solid Phase Peptide Synthesis: A Practical Approach*; Oxford University Press, 1999. https://doi.org/10.1093/oso/9780199637256.001.0001.

(61) Craik, D. J.; Fairlie, D. P.; Liras, S.; Price, D. The Future of Peptide-Based Drugs. *Chem. Biol. Drug Des.* **2013**, *81* (1), 136–147. https://doi.org/10.1111/cbdd.12055.

(62) Zhu, N.; Dong, F.; Shi, G.; Lao, X.; Zheng, H. HORDB a Comprehensive Database of Peptide Hormones. *Sci. Data* **2022**, *9*. https://doi.org/10.1038/s41597-022-01287-5.

(63) Uhlig, T.; Kyprianou, T.; Martinelli, F. G.; Oppici, C. A.; Heiligers, D.; Hills, D.; Calvo, X. R.; Verhaert, P. The Emergence of Peptides in the Pharmaceutical Business: From Exploration to Exploitation. *EuPA Open Proteomics* **2014**, *4*, 58–69. https://doi.org/10.1016/j.euprot.2014.05.003.

(64) Mba, I. E.; Nweze, E. I. Antimicrobial Peptides Therapy: An Emerging Alternative for Treating Drug-Resistant Bacteria. *Yale J. Biol. Med.* **2022**, *95* (4), 445–463.

(65) Vadevoo, S. M. P.; Gurung, S.; Lee, H.-S.; Gunassekaran, G. R.; Lee, S.-M.; Yoon, J.-W.; Lee, Y.-K.; Lee, B. Peptides as Multifunctional Players in Cancer Therapy. *Exp. Mol. Med.* **2023**, *55* (6), 1099–1109. https://doi.org/10.1038/s12276-023-01016-x.

(66) Fricker, L. D.; Devi, L. A. Orphan Neuropeptides and Receptors: Novel Therapeutic Targets. *Pharmacol. Ther.* **2018**, *185*, 26–33. https://doi.org/10.1016/j.pharmthera.2017.11.006.

(67) Pavlicevic, M.; Marmiroli, N.; Maestri, E. Immunomodulatory Peptides—A Promising Source for Novel Functional Food Production and Drug Discovery. *Peptides* **2022**, *148*, 170696. https://doi.org/10.1016/j.peptides.2021.170696.

(68) Rossino, G.; Marchese, E.; Galli, G.; Verde, F.; Finizio, M.; Serra, M.; Linciano, P.; Collina, S. Peptides as Therapeutic Agents: Challenges and Opportunities in the Green Transition Era. *Molecules* **2023**, *28* (20), 7165. https://doi.org/10.3390/molecules28207165.

(69) Biomatik. *7 Applications Of Peptide Synthesis*. Biomatik. https://www.biomatik.com/blog/applications-peptide-synthesis/ (accessed 2024-02-20).

(70) Boaro, A.; Ageitos, L.; Torres, M.; Bartoloni, F. H.; de la Fuente-Nunez, C. Light-Emitting Probes for Labeling Peptides. *Cell Rep. Phys. Sci.* **2020**, *1* (12), 100257. https://doi.org/10.1016/j.xcrp.2020.100257.

(71) Maity, D. Selected Peptide-Based Fluorescent Probes for Biological Applications. *Beilstein J. Org. Chem.* **2020**, *16*, 2971–2982. https://doi.org/10.3762/bjoc.16.247.

(72) Chen, H.-M.; Tsai, Y.-H.; Hsu, C.-Y.; Wang, Y.-Y.; Hsieh, C.-E.; Chen, J.-H.; Chang, Y.-S.; Lin, C.-Y. Peptide-Coated Bacteriorhodopsin-Based Photoelectric Biosensor for Detecting Rheumatoid Arthritis. *Biosensors* **2023**, *13* (10), 929. https://doi.org/10.3390/bios13100929.

(73) Francis, M. J. Recent Advances in Vaccine Technologies. *Vet. Clin. North Am. Small Anim. Pract.* **2018**, *48* (2), 231–241. https://doi.org/10.1016/j.cvsm.2017.10.002.

(74) Strimbu, K.; Tavel, J. A. What Are Biomarkers? *Curr. Opin. HIV AIDS* **2010**, *5* (6), 463–466. https://doi.org/10.1097/COH.0b013e32833ed177.

(75) Su, R.; Xin, S.; Zhou, X.; Liu, F.; Zhang, Y.; Deng, Y. Discovery and Validation of Glucose-Sensitive Peptide Biomarkers from Human Serum Albumin to Diagnose Type 2 Diabetes Mellitus. *Talanta* **2023**, *260*, 124574. https://doi.org/10.1016/j.talanta.2023.124574.

(76) Lee, P. Y.; Low, T. Y.; Jamal, R. Chapter Three - Probing the Endogenous Peptidomes of Cancer for Biomarkers: A New Endeavor. In *Advances in Clinical Chemistry*; Makowski, G. S., Ed.; Elsevier, 2019; Vol. 88, pp 67–89. https://doi.org/10.1016/bs.acc.2018.10.004.

(77) Mukherjee, S.; Perez, K. A.; Dubois, C.; Nisbet, R. M.; Li, Q.-X.; Varghese, S.; Jin, L.; Birchall, I.; Streltsov, V. A.; Vella, L. J.; McLean, C.; Barham, K. J.; Roberts, B. R.; Masters, C. L. Citrullination of Amyloid-β Peptides in Alzheimer's Disease. *ACS Chem. Neurosci.* **2021**, *12* (19), 3719–3732. https://doi.org/10.1021/acschemneuro.1c00474.

(78) Fekih-Zaghbib, S.; Ksouri, A.; Bouhaouala-Zahar, B. Differences in Fish Mucus Proteomes Identify Potential Antimicrobial Peptide Biomarkers. *Dev. Comp. Immunol.* **2023**, *145*, 104730. https://doi.org/10.1016/j.dci.2023.104730.

(79) Lee, S.; Xie, J.; Chen, X. Peptide-Based Probes for Targeted Molecular Imaging. *Biochemistry* **2010**, *49* (7), 1364–1376. https://doi.org/10.1021/bi901135x.

(80) Wang, W.; Hu, Z. Targeting Peptide-Based Probes for Molecular Imaging and Diagnosis. *Adv. Mater.* **2019**, *31* (45), 1804827. https://doi.org/10.1002/adma.201804827.

(81) SB Peptide. *Peptide fluorescent labeling - SB-PEPTIDE - Peptide engineering*. SB PEPTIDE. https://www.sb-peptide.com/peptide-service/peptide-modification/peptide-fluorescent-labeling/ (accessed 2024-03-26).

(82) Li, H.; Aneja, R.; Chaiken, I. Click Chemistry in Peptide-Based Drug Design. *Molecules* **2013**, *18* (8), 9797–9817. https://doi.org/10.3390/molecules18089797.

(83) Creative Peptides. *Fluorescence and Dye Labeled Peptides - Creative Peptides-Peptide Drug Discovery*. https://www.pepdd.com/services/fluorescence-and-dye-labeled-peptides.html (accessed 2024-03-26).

(84) Bio-IT World. *Useful Approaches for Labeling Peptides with Fluorescent Dyes*. Pubs - Bio-IT World. https://www.bio-itworld.com/pressreleases/2022/03/17/useful-approaches-for-labeling-peptides-with-fluorescent-dyes (accessed 2024-03-26).

(85) Fan, Z.; Chang, Y.; Cui, C.; Sun, L.; Wang, D. H.; Pan, Z.; Zhang, M. Near Infrared Fluorescent Peptide Nanoparticles for Enhancing Esophageal Cancer Therapeutic Efficacy. *Nat. Commun.* **2018**, *9* (1), 2605. https://doi.org/10.1038/s41467-018-04763-y.

(86) Kuznetsov, A.; Arukuusk, P.; Härk, H.; Juronen, E.; Ustav, M.; Langel, Ü.; Järv, J. ACE2 Peptide Fragment Interaction with Different S1 Protein Sites. *Int. J. Pept. Res. Ther.* **2022**, *28* (1), 7. https://doi.org/10.1007/s10989-021-10324-7.

(87) Fountain, J. H.; Kaur, J.; Lappin, S. L. Physiology, Renin Angiotensin System. In *StatPearls*; StatPearls Publishing: Treasure Island (FL), 2024.

(88) National Library of Medicine. *ACE2 angiotensin converting enzyme 2 [Homo sapiens (human)] - Gene - NCBI*. https://www.ncbi.nlm.nih.gov/gene/59272 (accessed 2024-04-01).

(89) Lambert, D. W.; Yarski, M.; Warner, F. J.; Thornhill, P.; Parkin, E. T.; Smith, A. I.; Hooper, N. M.; Turner, A. J. Tumor Necrosis Factor-α Convertase (ADAM17) Mediates Regulated Ectodomain Shedding of the Severe-Acute Respiratory Syndrome-Coronavirus (SARS-CoV) Receptor, Angiotensin-Converting Enzyme-2 (ACE2)*. *J. Biol. Chem.* **2005**, *280* (34), 30113–30119. https://doi.org/10.1074/jbc.M505111200.

(90) Alenina, N.; Bader, M. ACE2 in Brain Physiology and Pathophysiology: Evidence from Transgenic Animal Models. *Neurochem. Res.* **2019**, *44* (6), 1323–1329. https://doi.org/10.1007/s11064-018-2679-4.

(91) Angiotensin-Converting Enzyme 2. *Wikipedia*; 2024.

(92) *Overview of ELISA - EE*. https://www.thermofisher.com/tr/en/home/life-science/protein-biology/protein-biology-learning-center/protein-biology-resource-library/pierce-protein-methods/overview-elisa.html (accessed 2024-04-11).

(93) Hong, J. S.; Shamim, A.; Atta, H.; Nonnecke, E. B.; Merl, S.; Patwardhan, S.; Manell, E.; Gunes, E.; Jordache, P.; Chen, B.; Lu, W.; Shen, B.; Dionigi, B.; Kiran, R. P.; Sykes, M.; Zorn, E.; Bevins, C. L.; Weiner, J. Application of Enzyme-Linked Immunosorbent Assay to Detect Antimicrobial Peptides in Human Intestinal Lumen. *J. Immunol. Methods* **2024**, *525*, 113599. https://doi.org/10.1016/j.jim.2023.113599.

(94) Fnu, P. I. J.; Hassan, M. T.-A.; Yaroshuk, T.; Ai, Y.; Chen, H. Absolute Quantitation of Peptides and Proteins by Coulometric Mass Spectrometry after Derivatization. *Int. J. Mass Spectrom.* **2024**, *495*, 117153. https://doi.org/10.1016/j.ijms.2023.117153.

(95) Boroumand, M.; Grassi, V. M.; Castagnola, F.; De-Giorgio, F.; d'Aloja, E.; Vetrugno, G.; Pascali, V. L.; Vincenzoni, F.; Iavarone, F.; Faa, G.; Castagnola, M. Estimation of Postmortem Interval Using Top-down HPLC–MS Analysis of Peptide Fragments in Vitreous Humour: A Pilot Study. *Int. J. Mass Spectrom.* **2023**, *483*, 116952. https://doi.org/10.1016/j.ijms.2022.116952.

(96) Pritchard, C.; Torma, F. A.; Hopley, C.; Quaglia, M.; O'Connor, G. Investigating Microwave Hydrolysis for the Traceable Quantification of Peptide Standards Using Gas Chromatography–Mass Spectrometry. *Anal. Biochem.* **2011**, *412* (1), 40–46. https://doi.org/10.1016/j.ab.2010.12.015.

(97) Han, L.; Zhu, X.; Zhang, D.; Liu, H.; Sun, B. Peptide-Based Molecularly Imprinted Polymer: A Visual and Digital Platform for Specific Recognition and Detection of Ethyl Carbamate. *ACS Sens.* **2023**, *8* (2), 694–703. https://doi.org/10.1021/acssensors.2c02197.

(98) Liu, X.; Zhang, X.; Fu, Z.; Cheng, X.; Wang, L.; Hu, L. Mesoporous Molecularly Imprinted Nanoparticles with Peptide Mimics for the Detection of Phenolic Compounds. *Anal. Chim. Acta* **2023**, *1250*, 340970. https://doi.org/10.1016/j.aca.2023.340970.

(99) Resina, L.; Alemán, C.; Ferreira, F. C.; Esteves, T. Protein-Imprinted Polymers: How Far Have "Plastic Antibodies" Come? *Biotechnol. Adv.* **2023**, *68*, 108220. https://doi.org/10.1016/j.biotechadv.2023.108220.

(100) Khumsap, T.; Corpuz, A.; Thai Nguyen, L. Epitope-Imprinted Polymers: Applications in Protein Recognition and Separation. *RSC Adv.* **2021**, *11* (19), 11403–11414. https://doi.org/10.1039/D0RA10742E.

(101) Teixeira, S. P. B.; Reis, R. L.; Peppas, N. A.; Gomes, M. E.; Domingues, R. M. A. Epitope-Imprinted Polymers: Design Principles of Synthetic Binding Partners for Natural Biomacromolecules. *Sci. Adv. 7* (44), eabi9884. https://doi.org/10.1126/sciadv.abi9884.

(102) Zhang, Y.; Deng, C.; Liu, S.; Wu, J.; Chen, Z.; Li, C.; Lu, W. Active Targeting of Tumors through Conformational Epitope Imprinting. *Angew. Chem. Int. Ed.* **2015**, *54* (17), 5157–5160. https://doi.org/10.1002/anie.201412114.

(103) Rachkov, A.; Minoura, N. Recognition of Oxytocin and Oxytocin-Related Peptides in Aqueous Media Using a Molecularly Imprinted Polymer Synthesized by the Epitope Approach. *J. Chromatogr. A* **2000**, *889* (1), 111–118. https://doi.org/10.1016/S0021-9673(00)00568-9.

(104) Canfarotta, F.; Czulak, J.; Betlem, K.; Sachdeva, A.; Eersels, K.; Grinsven, B. van; Cleij, T. J.; Peeters, M. A Novel Thermal Detection Method Based on Molecularly Imprinted Nanoparticles as Recognition Elements. *Nanoscale* **2018**, *10* (4), 2081–2089. https://doi.org/10.1039/C7NR07785H.

(105) Di Giulio, T.; Barca, A.; Verri, T.; De Gennaro, M.; Giancane, G.; Mazzotta, E.; Malitesta, C. Molecular Imprinting Based on Metal-Ion Mediated Recognition: Electrosynthesis of Artificial Receptors for the Selective Detection of Peptides. *Sens. Actuators B Chem.* **2023**, *383*, 133589. https://doi.org/10.1016/j.snb.2023.133589.

(106) Yang, J. C.; Lee, J.; Lim, S. J.; Kwak, G.; Park, J. Molecularly Imprinted Chalcone-Branched Polyimide-Based Chemosensors with Stripe Nanopatterns for the Detection of Melittin. *ACS Sens.* **2023**, *8* (6), 2298–2308. https://doi.org/10.1021/acssensors.3c00341.

(107) Hoshino, Y.; Kodama, T.; Okahata, Y.; Shea, K. J. Peptide Imprinted Polymer Nanoparticles: A Plastic Antibody. *J. Am. Chem. Soc.* **2008**, *130* (46), 15242–15243. https://doi.org/10.1021/ja8062875.

(108) Tan, F.; Zhai, M.; Meng, X.; Wang, Y.; Zhao, H.; Wang, X. Hybrid Peptide-Molecularly Imprinted Polymer Interface for Electrochemical Detection of Vancomycin in Complex Matrices. *Biosens. Bioelectron.* **2021**, *184*, 113220. https://doi.org/10.1016/j.bios.2021.113220.

(109) Lee, M.-H.; Lin, C.-C.; Thomas, J. L.; Chen, C.-Y.; Chen, C.-Y.; Yang, C.-H.; Lin, H.-Y. Sensing a SARS-CoV-2 Spike Peptide Using a Titanium Carbide-Doped Imprinted Polymer-Coated Extended-Gate Field Effect Transistor. *Sens. Bio-Sens. Res.* **2023**, *41*, 100577. https://doi.org/10.1016/j.sbsr.2023.100577.

(110) Amanda Quiroga. *Cyclic Voltammetry*. Chemistry LibreTexts. https://chem.libretexts.org/Bookshelves/Analytical_Chemistry/Supplemental_Modules_(Analytical_Chemistry)/Instrumentation_and_Analysis/Cyclic_Voltammetry (accessed 2024-03-08).

(111) Bard, A. J.; Faulkner, L. R. *Electrochemical Methods: Fundamentals and Applications*, 2. edition.; Wiley: New York Weinheim, 2001.

(112) Kissinger, P. T.; Heineman, W. R. *Laboratory Techniques in Electroanalytical Chemistry*, 2nd ed., rev.expanded.; Marcel Dekker, Inc.: New York, 1996.

(113) Gamry Instruments. *Cyclic Voltammetry: Electrochemical Technique - Gamry Instruments Gamry Instruments*. https://www.gamry.com/cyclic-voltammetry/ (accessed 2024-03-07).

(114) Dr. Chris Bracher; Harry Robson. *Cyclic Voltammetry Uses | How to Read a Voltammogram*. Ossila. https://www.ossila.com/pages/cyclic-voltammetry-applications (accessed 2024-03-07).

(115) Lin, C.-H.; Lin, J.-H.; Chen, C.; Ito, Y.; Luo, S.-C. Conducting Polymer-Based Sensors for Food and Drug Analysis. *J. Food Drug Anal.* **2021**, *29*, 544–558. https://doi.org/10.38212/2224-6614.3374.

(116) M.S. Gião; M.I. Montenegro; M.J. Vieira. Monitoring Biofilm Formation by Using Cyclic Voltammetry : Effect of the Experimental Conditions on Biofilm Removal and Activity.

(117) Kang, J.; Kim, T.; Tak, Y.; Lee, J.-H.; Yoon, J. Cyclic Voltammetry for Monitoring Bacterial Attachment and Biofilm Formation. *J. Ind. Eng. Chem.* **2012**, *18* (2), 800–807. https://doi.org/10.1016/j.jiec.2011.10.002.

(118) *Cyclic Voltammetry: A Electro Chemical Technique for Environmental Scientists - ChemSpectro*. https://chemspectro.com/cyclic-voltammetry-a-electro-chemical-technique-for-environmental-scientists/ (accessed 2024-03-07).

(119) Wang, H.-W.; Bringans, C.; Hickey, A. J. R.; Windsor, J. A.; Kilmartin, P. A.; Phillips, A. R. J. Cyclic Voltammetry in Biological Samples: A Systematic Review of Methods and Techniques Applicable to Clinical Settings. *Signals* **2021**, *2* (1), 138–158. https://doi.org/10.3390/signals2010012.

(120) Wang, J.; John Wiley & Sons. *Analytical Electrochemistry (Second Edition)*, 2nd ed.; Wiley-VCH: New York, 2000.

(121) Simões, F. R.; Xavier, M. G. 6 - Electrochemical Sensors. In *Nanoscience and its Applications*; Da Róz, A. L., Ferreira, M., de Lima Leite, F., Oliveira, O. N., Eds.; Micro and Nano Technologies; William Andrew Publishing, 2017; pp 155–178. https://doi.org/10.1016/B978-0-323-49780-0.00006-5.

(122) Venton, B. J.; DiScenza, D. J. Chapter 3 - Voltammetry. In *Electrochemistry for Bioanalysis*; Patel, B., Ed.; Elsevier, 2020; pp 27–50. https://doi.org/10.1016/B978-0-12-821203-5.00004-X.

(123) BASi. *Pulse Voltammetric Techniques*. https://www.basinc.com/manuals/EC_epsilon/Techniques/Pulse/pulse (accessed 2024-04-24).

(124) Alex Peroff. *Differential Pulse Voltammetry (DPV)*. Pine Research Instrumentation Store. https://pineresearch.com/shop/kb/software/methods-and-techniques/voltammetric-methods/differential-pulse-voltammetry-dpv/ (accessed 2024-03-12).

(125) Cadence PCB solutions. *Differential Pulse Voltammetry Explained*. https://resources.pcb.cadence.com/blog/2021-differential-pulse-voltammetry-explained (accessed 2024-03-12).

(126) Singh, M.; Kushwaha, A.; Gupta, N.; Singh, S.; Singh, A. Synthesis and Characterization of Antipyrine Imprinted Polymers and Their Application for Sustained Release. *Polym. Bull.* **2018**, *75*. https://doi.org/10.1007/s00289-018-2326-x.

(127) Mahmoud, A.; El-Wekil, M.; Mahnashi, M.; Ali, M.; Alkahtani, S. Modification of N,S Co-Doped Graphene Quantum Dots with p-Aminothiophenol-Functionalized Gold Nanoparticles for Molecular Imprint-Based Voltammetric Determination of the Antiviral Drug Sofosbuvir. *Microchim. Acta* **2019**, *186*. https://doi.org/10.1007/s00604-019-3647-7.

(128) Gerard Macias. *Differential Pulse Voltammetry - Macias Sensors*. https://maciassensors.com/differential-pulse-voltammetry/ (accessed 2024-03-12).

(129) Kidakova, A.; Boroznjak, R.; Reut, J.; Öpik, A.; Saarma, M.; Syritski, V. Molecularly Imprinted Polymer-Based SAW Sensor for Label-Free Detection of Cerebral Dopamine Neurotrophic Factor Protein. *Sens. Actuators B Chem.* **2020**, *308*, 127708. https://doi.org/10.1016/j.snb.2020.127708.

(130) Umpleby, R. J.; Baxter, S. C.; Chen, Y.; Shah, R. N.; Shimizu, K. D. Characterization of Molecularly Imprinted Polymers with the Langmuir−Freundlich Isotherm. *Anal. Chem.* **2001**, *73* (19), 4584–4591. https://doi.org/10.1021/ac0105686.

(131) Thomas C. Freeman. *PepDraw*. PepDraw. https://pepdraw.com/ (accessed 2024-01-24).

(132) Morris, G. M.; Lim-Wilby, M. Molecular Docking. In *Molecular Modeling of Proteins*; Kukol, A., Ed.; Methods Molecular Biology™; Humana Press: Totowa, NJ, 2008; pp 365–382. https://doi.org/10.1007/978-1-59745-177-2_19.

(133) Weng, G.; Wang, E.; Chen, F.; Sun, H.; Wang, Z.; Hou, T. Assessing the Performance of MM/PBSA and MM/GBSA Methods. 9. Prediction Reliability of Binding Affinities and Binding Poses for Protein–Peptide Complexes. *Phys. Chem. Chem. Phys.* **2019**, *21* (19), 10135–10145. https://doi.org/10.1039/C9CP01674K.

(134) Ayankojo, A. G.; Boroznjak, R.; Reut, J.; Tuvikene, J.; Timmusk, T.; Syritski, V. Electrochemical Sensor Based on Molecularly Imprinted Polymer for Rapid Quantitative Detection of Brain-Derived Neurotrophic Factor. *Sens. Actuators B Chem.* **2023**, *397*, 134656. https://doi.org/10.1016/j.snb.2023.134656.

(135) Nguyen, V. B. C.; Reut, J.; Rappich, J.; Hinrichs, K.; Syritski, V. Molecularly Imprinted Polymer-Based Electrochemical Sensor for the Detection of Azoxystrobin in Aqueous Media. *Polymers* **2024**, *16* (10), 1394. https://doi.org/10.3390/polym16101394.

(136) Latour, R. A. The Langmuir Isotherm: A Commonly Applied but Misleading Approach for the Analysis of Protein Adsorption Behavior. *J. Biomed. Mater. Res. A* **2015**, *103* (3), 949–958. https://doi.org/10.1002/jbm.a.35235.

(137) Carpenter, G.; Cohen, S. Epidermal Growth Factor. *J. Biol. Chem.* **1990**, *265* (14), 7709–7712. https://doi.org/10.1016/S0021-9258(19)38983-5.

(138) *How the Sequencing of Amino Acids in Insulin Revealed the Structure of Proteins | Amino Acids Explained | Amino Acids*. Ajinomoto Group Global Website - Eat Well, Live Well. https://www.ajinomoto.com/amino-acids/how-the-sequencing-of-amino-acids-in-insulin-revealed-the-structure-of-proteins (accessed 2024-05-25).

(139) Zidarič, T.; Majer, D.; Maver, T.; Finšgar, M.; Maver, U. The Development of an Electropolymerized, Molecularly Imprinted Polymer (MIP) Sensor for Insulin Determination Using Single-Drop Analysis. *Analyst* **2023**, *148* (5), 1102–1115. https://doi.org/10.1039/D2AN02025D.

(140) Zhang, Z.; Ma, L.; Yuan, H.; Chen, Z.; Lv, Y. Solid-Phase Screening and Synthesis of Molecularly Imprinted Nanoparticles for Selective Recognition and Detection of Brain Natriuretic Peptide. *Adv. Healthc. Mater.* **2023**, *12* (13), 2300146. https://doi.org/10.1002/adhm.202300146.

Appendix 1

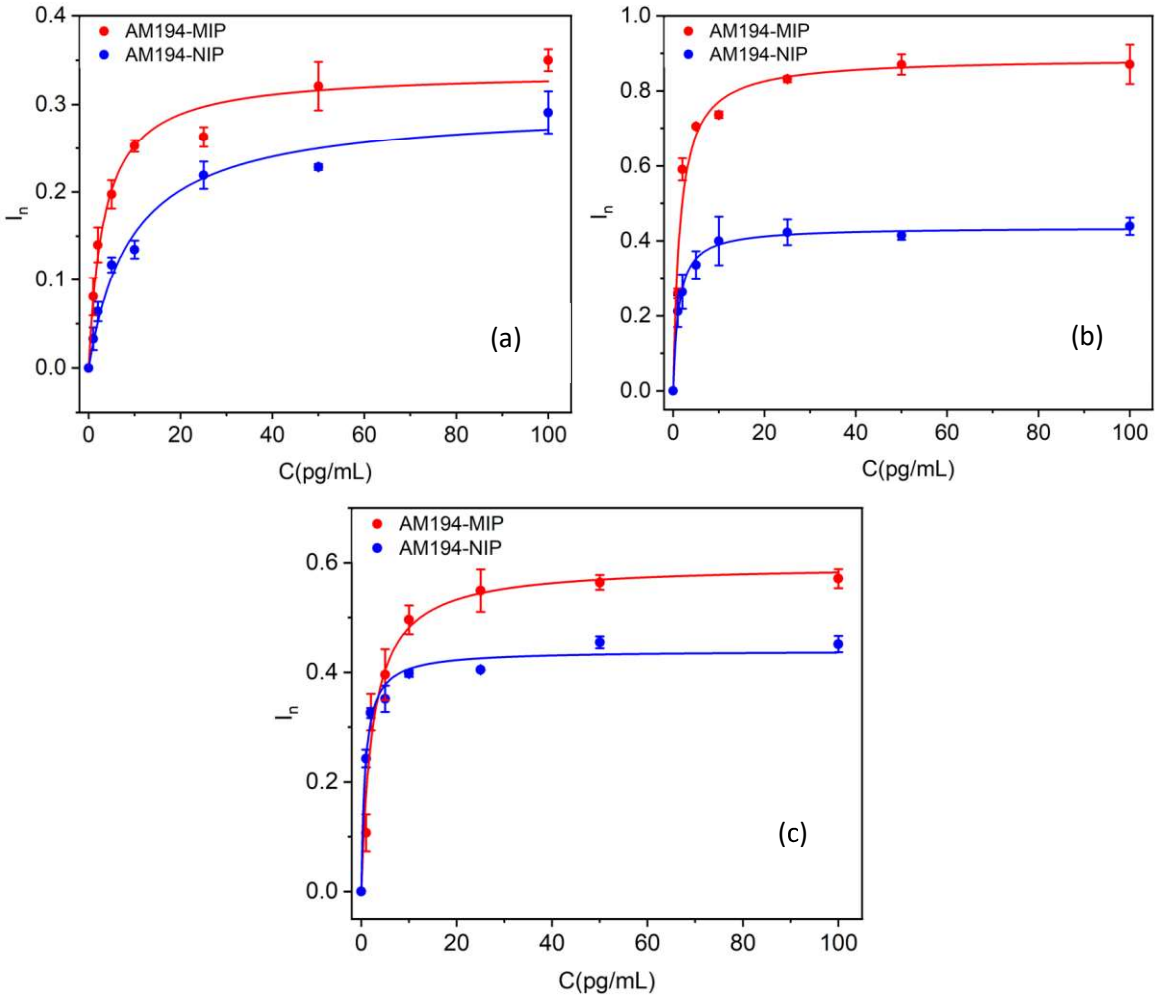

Figure A. AM194 adsorption isotherms on the AM194-MIP (red) and AM194-NIP (blue) synthesized galvanostatically at 500 µA during 5.6 s from solutions having different concentrations of DA (a) 2.5 mM, (b) 5 mM and (c) 10 mM. The lines show fits to Langmuir adsorption model.

Appendix 2

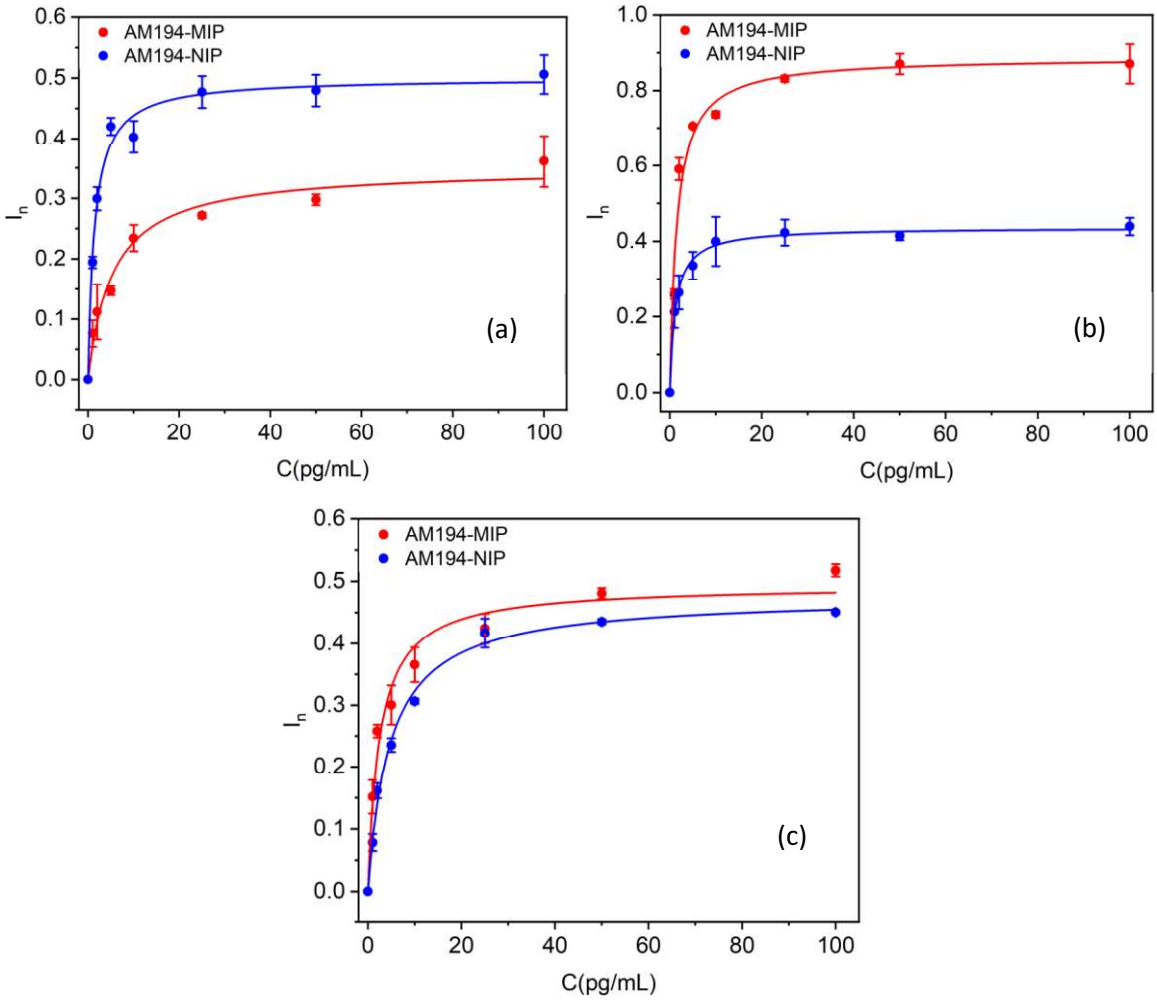

Figure B. AM194 adsorption isotherms on the AM194-MIP (red) and AM194-NIP (blue) having concentration of DA 5 mM and synthesized galvanostatically at 500 µA during different polymerization times (a) 2.8, (b) 5.6 and (c) 8.4 s. The lines show fits to Langmuir adsorption model.

Lihtlitsents lõputöö reprodutseerimiseks ja lõputöö üldsusele kättesaadavaks tegemiseks[1]

Mina David Tsaregorodtsev,

1. Annan Tallinna Tehnikaülikoolile tasuta loa (lihtlitsentsi) enda loodud teose "Molecular imprinting of ACE2 Peptide Fragment: towards Development Peptide-Selective Electrochemical", mille juhendajad on Vitali Sõritski ja Jekaterina Reut,

1.1 reprodutseerimiseks lõputöö säilitamise ja elektroonse avaldamise eesmärgil, sh Tallinna Tehnikaülikooli raamatukogu digikogusse lisamise eesmärgil kuni autoriõiguse kehtivuse tähtaja lõppemiseni;

1.2 üldsusele kättesaadavaks tegemiseks Tallinna Tehnikaülikooli veebikeskkonna kaudu, sealhulgas Tallinna Tehnikaülikooli raamatukogu digikogu kaudu kuni autoriõiguse kehtivuse tähtaja lõppemiseni.

2. Olen teadlik, et käesoleva lihtlitsentsi punktis 1 nimetatud õigused jäävad alles ka autorile.

3. Kinnitan, et lihtlitsentsi andmisega ei rikuta teiste isikute intellektuaalomandi ega isikuandmete kaitse seadusest ning muudest õigusaktidest tulenevaid õigusi.

27.05.2024

[1] *Lihtlitsents ei kehti juurdepääsupiirangu kehtivuse ajal vastavalt üliõpilase taotlusele lõputööle juurdepääsupiirangu kehtestamiseks, mis on allkirjastatud teaduskonna dekaani poolt, välja arvatud ülikooli õigus lõputööd reprodutseerida üksnes säilitamise eesmärgil. Kui lõputöö on loonud kaks või enam isikut oma ühise loomingulise tegevusega ning lõputöö kaas- või ühisautor(id) ei ole andnud lõputööd kaitsvale üliõpilasele kindlaksmääratud tähtajaks nõusolekut lõputöö reprodutseerimiseks ja avalikustamiseks vastavalt lihtlitsentsi punktidele 1.1. ja 1.2, siis lihtlitsents nimetatud tähtaja jooksul ei kehti.*